

From a P₄ Butterfly Scaffold to *cyclo*- and *catena*-P₄ Units.

Julian Müller, Gábor Balázs, and Manfred Scheer*

Table of content

1.	Synthesis and Characterization	2
1.1.	Synthesis of $[\{\text{Cp}^{\text{**}}\text{Fe}(\text{CO})_2\}_2(\mu_3, \eta^{4:1:1}\text{-P}_4)\{\text{CymRu}\}][\text{PF}_6]_2$ (2).....	2
1.2.	Synthesis of $[\{\text{Cp}^{\text{**}}\text{Fe}(\text{CO})_2\}_2(\mu_3, \eta^{4:1:1}\text{-P}_4)(\text{Cp}^*\text{Rh})][\text{PF}_6]_2$ (3)	3
1.3.	Synthesis of $[\{\text{Cp}^{\text{**}}\text{Fe}(\text{CO})_2\}_2(\mu_3, \eta^{4:1:1}\text{-P}_4)(\text{Cp}^*\text{Ir})][\text{PF}_6]_2$ (4)	4
1.4.	Synthesis of $[\{\text{Cp}^{\text{**}}\text{Fe}(\text{CO})_2\}_2(\mu_3, \eta^{4:1:1}\text{-P}_4)(\text{Cp}^*\text{Ru})][\text{PF}_6]$ (5)	4
1.5.	Synthesis of $[\{\text{Cp}^{\text{**}}\text{Fe}(\text{CO})_2\}\{\text{Cp}^{\text{**}}\text{Fe}(\text{CO})\}(\mu_3, \eta^{4:2:1}\text{-P}_4)(\text{Cp}^*\text{Ru})][\text{PF}_6]$ (6)	5
2.	Crystallographic Details	6
3.	¹ H NMR and ³¹ P NMR Spectroscopy	11
4.	Computational Details	25
5.	Literature:	27

1. Synthesis and Characterization

General Remarks:

All manipulations were performed with rigorous exclusion of oxygen and moisture using Schlenk-type glassware on a dual manifold Schlenk line with Argon inert gas or glove box filled with N₂ or Ar containing a high-capacity recirculator (<0.1 ppm O₂). All solvents except were dried using a MB SPS-800 device of company MBRAUN, degassed and saturated with argon. Mass spectrometry was performed using a Waters Micromass LCT (ESI-MS) and a Jeol AccuTOF GCX (LIFDI-MS), respectively. Elemental analysis (CHN) was determined using a Vario micro cube. Infrared spectroscopy was performed using a Thermo Scientific Nicolet iS5 spectrometer.

Ti[PF₆] (97%) was purchased by abcr and was used without further purification. Compound [Cp^{'''}Fe(CO)₂]₂(μ,η^{1:1}-P₄)]^[1] (**1**) and [Cp^{*}Ru(NCCH₃)₃][PF₆]^[2] were synthesized according to literature known procedures.

1.1. Synthesis of [Cp^{'''}Fe(CO)₂]₂(μ₃,η^{4:1:1}-P₄){CymRu}[PF₆]₂ (**2**)

The reaction is best performed in the absence of light. Although the ³¹P NMR spectra of the reaction mixtures (with light and without light) are comparable, crystallization works much better when light is excluded.

0.100 g of compound **1** (0.123 mmol, 1eq), 0.038 g of [CymRuCl₂]₂ (0.061 mmol, 0.5eq) and 0.129 g Ti[PF₆] (0.368 mmol, 3eq) are suspended in 20 ml CH₂Cl₂. The mixture is stirred for 16 h at room temperature during which an off-white precipitate is formed. The suspension is filtered over diatomaceous earth to give a dark yellow solution. Crystals of **2** can be obtained by layering a CH₂Cl₂ solution under pentane.

Yield: 0.080 g (0,060 mmol, 49%)

Analytical data of **2**:

NMR (CD ₂ Cl ₂ , 298 K)	¹ H: δ [ppm] = 1.33 (s, 18, -(C ₄ H ₉)), 1.35 (d, ³ J _{HH} = 6.93 Hz, 6H, MeC ₆ H ₄ CH(CH ₃) ₂) 1.45 (s, 36H, -(C ₄ H ₉) ₂), 2.59 (s, 3H, CH ₃ C ₆ H ₄ ⁱ Pr), 2.84 (sept, ³ J _{HH} = 6.90 Hz, 1H, MeC ₆ H ₄ CH(CH ₃) ₂), 5.66 (m, 4H, C ₅ H ₂ ⁱ Bu ₃). 6.71 (m, 4H, MeC ₆ H ₄ ⁱ Pr). ³¹ P{ ¹ H}: δ [ppm] = 148.9 (m, 2P), 102.9 (m, 2P), -143.7 (sept. 2P, ¹ J _{PF} = 710 Hz). Coupling constants of the cation are summarized in Table S2.
IR (CH ₂ Cl ₂)	$\tilde{\nu}$ [cm ⁻¹] = 2037.4 (s), 1997.3 (vs)
Elemental analysis (C ₄₈ H ₇₂ F ₁₂ Fe ₂ O ₄ P ₆ Ru · (C ₅ H ₁₂) _{0.2})	Calculated: C 43.46, H 5.54 Found: C 43.38, H 5.24.

Mass spectrometry (ESI, CH₃CN)

m/z: 1208.2 (< 1%) [M + PF₆ - CO + NCCH₃]⁺, 1195.2 (3%) [M + PF₆]⁺, 705.1 (22%) [M - Cp^{'''}Fe(CO)₂]⁺, 525.1 (100%) [M]²⁺, 399.2 (6%) [Cp^{'''}Fe(CO)(NCCH₃)₂]⁺, 386.2 (46%) [Cp^{'''}Fe(CO)₂(NCCH₃)]⁺, 373.1 (8%) [Cp^{'''}Fe(CO)₃]⁺, 358.2 (20%) [Cp^{'''}Fe(CO)(NCCH₃)]⁺, 345.1 (6%) [Cp^{'''}Fe(CO)₂]⁺, 330.2 (60%) [Cp^{'''}Fe(NCCH₃)]⁺, 317.2 (2%) [Cp^{'''}Fe(CO)]⁺, 289.2 (2%) [Cp^{'''}Fe]⁺, 144.8 [PF₆]⁻.

1.2. Synthesis of [(Cp^{'''}Fe(CO)₂)₂(μ₃,η^{4:1:1}-P₄)(Cp^{*}Rh)][PF₆]₂ (**3**)

0.100 g of compound **1** (0.123 mmol, 1eq), 0.054 g of [Cp^{*}RhBr₂]₂ (0.068 mmol, 0.55eq) and 0.129 mg Ti[PF₆] (0.368 mg, 3eq) are suspended in 10 ml of CH₂Cl₂ and stirred for 16 h at room temperature. The mixture is filtered over diatomaceous earth and the solvent of the filtrate is removed in vacuum to give **3** as a dark orange powder. Crystals of **3** are obtained by layering a CH₂Cl₂ solution under hexane.

Yield: 0.086g (0,064 mmol, 52%)

Analytical data of **3**:

NMR (CD₂Cl₂, 298 K)

¹H: δ [ppm] = 1.36 (s, 18H, -(C₄H₉)), 1.48 (s, 36H, -(C₄H₉)₂), 2.46 (s, 15H, C₅(CH₃)₅) 5.73 (m, 4H, C₅H₂¹Bu₃).

³¹P{¹H}: δ [ppm] = 129.8 (m, 2P), 121.1 (m, 2P), -143.7 (sept. 2P, ¹J_{PF} = 711 Hz).

Coupling constants of the cation are summarized in Table S3.

IR (CH ₂ Cl ₂)	$\tilde{\nu}$ [cm ⁻¹] = 2004 (vs), 2042 (vs)
Elemental analysis (C ₄₈ H ₇₃ F ₁₂ Fe ₂ O ₄ P ₆ Rh · (CH ₂ Cl ₂) ₂)	Calculated: C 39.71, H 5.13 Found: C 40.27, H 4.99.
Mass spectrometry (ESI, CH ₃ CN)	m/z: 1197.2 (5%) [M + PF ₆] ⁺ , 707.1 (100%) [M - Cp ^{'''} Fe(CO) ₂] ⁺ , 526.1 (51%) [M] ²⁺ , 386.2 (86%) [Cp ^{'''} Fe(CO) ₂ (NCCH ₃)] ⁺ , 358.2 (11%) [Cp ^{'''} Fe(CO)(NCCH ₃)] ⁺ , 345.1 (7%) [Cp ^{'''} Fe(CO) ₂] ⁺ , 330.2 (23%) [Cp ^{'''} Fe(NCCH ₃)] ⁺ , 317.2 (1%) [Cp ^{'''} Fe(CO)] ⁺ , 144.8 [PF ₆] ⁻ .

Analytical data of the side product:

NMR (CD₂Cl₂, 298 K)

³¹P{¹H}: δ [ppm] = 201.7 (m, 2P), 157.7 (m, 1P), 125.7 (m, 1P),).

Coupling constants are summarized in Table S4.

1.3. Synthesis of $[\{\text{Cp}^{\text{***}}\text{Fe}(\text{CO})_2\}_2(\mu_3, \eta^{4:1:1}\text{-P}_4)(\text{Cp}^*\text{Ir})][\text{PF}_6]_2$ (**4**)

0.100 g of compound **1** (0.123 mmol, 1eq), 0.049 g of $[\text{Cp}^*\text{IrCl}_2]_2$ (0.061 mmol, 0.5eq) and 0.129 g $\text{Ti}[\text{PF}_6]$ (0.368 mmol, 3eq) are transferred to a Young-tube and suspended in 20 ml CH_3CN . The mixture is treated in the ultrasonic bath for 16 h during which an off-white precipitate is formed. After evaporating the solvent, the residue is washed several times with thf which was rejected afterwards. The remaining residue is taken up in CH_2Cl_2 and filtered over diatomaceous earth. Evaporation of the solvent gives analytically pure **4** as a dark yellow powder. Crystals of **4** can be obtained by layering a CH_2Cl_2 solution under hexane.

Yield: 0.093g (0,065 mmol, 53%)

Analytical data of **4**:

NMR (CD_3CN , 298 K)	^1H : δ [ppm] = 1.35 (s, 18H, $-(\text{C}_4\text{H}_9)$), 1.46 (s, 36H, $-(\text{C}_4\text{H}_9)_2$), 2.64 (s, 15H, $\text{C}_5(\text{CH}_3)_5$), 5.79 (m br, 4H, $\text{C}_5\text{H}_2^t\text{Bu}_3$). $^{31}\text{P}\{^1\text{H}\}$: δ [ppm] = 62.2 (m, 2P), 102.3 (m, 2P), -143.7 (sept. 2P, $^1J_{\text{PF}} = 706$ Hz). Coupling constants of the cation are summarized in Table S5.
NMR (CD_2Cl_2 , 298 K)	$^{31}\text{P}\{^1\text{H}\}$: δ [ppm] = 60.5 (m, 2P), 107.1 (m, 2P), -143.6 (sept. 2P, $^1J_{\text{PF}} = 706$ Hz).
IR (CH_2Cl_2)	$\tilde{\nu}$ [cm^{-1}] = 2003 (vs), 2041 (vs)
Elemental analysis ($\text{C}_{48}\text{H}_{73}\text{F}_{12}\text{Fe}_2\text{O}_4\text{P}_6\text{Ir} \cdot (\text{CH}_2\text{Cl}_2)_{2.5}$)	Calculated: C 36.89, H 4.78 Found: C 37.23, H 4.54.
Mass spectrometry (ESI, CH_3CN)	m/z: 1287.3 (1%) $[\text{M} + \text{PF}_6]^+$, 797.2 (22%) $[\text{M} - (\text{Cp}^{\text{***}}\text{Fe}(\text{CO})_2)]^+$, 571.1 (100%) $[\text{M}]^{2+}$, 399.4 (15%) $[\text{Cp}^{\text{***}}\text{Fe}(\text{CO})(\text{NCCH}_3)_2]^+$, 387.4 (21%) $[\text{Cp}^{\text{***}}\text{Fe}(\text{CO})_2(\text{NCCH}_3)]^+$, 358.4 (14%) $[\text{Cp}^{\text{***}}\text{Fe}(\text{CO})(\text{NCCH}_3)]^+$

1.4. Synthesis of $[\{\text{Cp}^{\text{***}}\text{Fe}(\text{CO})_2\}_2(\mu_3, \eta^{4:1:1}\text{-P}_4)(\text{Cp}^*\text{Ru})][\text{PF}_6]$ (**5**)

In the absence of light are 0.200 g of compound **1** (0.246 mmol, 1eq) and 0.260 g of $[\text{Cp}^*\text{Ru}(\text{NCCH}_3)_3][\text{PF}_6]$ (0.516 mmol, 2.1eq) suspended in 15 ml of CH_2Cl_2 and stirred for 16 h at room temperature. The solvent is removed in vacuum and the residue is first washed with hexane and then taken up in CH_2Cl_2 and filtered over diatomaceous earth. Drying the CH_2Cl_2 solution in vacuum gives **5** as a red powder.

Yield: 0.241 g (0,201 mmol, 82%)

Analytical data of **5**:

NMR (CD_2Cl_2 , 298 K)	^1H : δ [ppm] = 1.34 (s br, 18, $-(\text{C}_4\text{H}_9)$), 1.47 (s, 36H, $-(\text{C}_4\text{H}_9)_2$), 2.27 (s, 15H, $\text{C}_5(\text{CH}_3)_5$), 5.34 (m, br, 4H, $\text{C}_5\text{H}_2^t\text{Bu}_3$).
---	--

	$^{31}\text{P}\{^1\text{H}\}$: δ [ppm] = 51.6 (m, 2P), 82.0 (m, 2P), -143.7 (sept. 2P, $^1J_{\text{PF}} = 710$ Hz). Coupling constants of the cation are summarized in Table S6.
IR (CH_2Cl_2)	$\tilde{\nu}$ [cm^{-1}] = 1990 (s), 2030 (s)
Elemental analysis ($\text{C}_{48}\text{H}_{73}\text{F}_6\text{Fe}_2\text{O}_4\text{P}_5\text{Ru}_1 \cdot (\text{C}_7\text{H}_8)_{0.66}$)	Calculated: C 50.32, H 6.28 Found: C 50.77, H 6.09.
Mass spectrometry (ESI, CH_3CN)	m/z: 1051.2 (100%) [M] ⁺ , 1023.2 (10%) [$\text{M} - \text{CO}$] ⁺

1.5. Synthesis of $[\{\text{Cp}^*\text{Fe}(\text{CO})_2\}\{\text{Cp}^*\text{Fe}(\text{CO})\}(\mu_3, \eta^{4:2:1}\text{-P}_4)(\text{Cp}^*\text{Ru})][\text{PF}_6]$ (**6**)

0.200 g of compound **1** (0.246 mmol, 1eq) and 0.260 g of $[\text{Cp}^*\text{Ru}(\text{NCCH}_3)_3][\text{PF}_6]$ (0.516 mmol, 2.1eq) are suspended in 15 ml of CH_2Cl_2 and stirred for 3 days at room temperature. The solvent is removed in vacuum and the residue is first washed with toluene and then taken up in ortho-difluorobenzene and filtered over diatomaceous earth. Drying the solution in vacuum gives a red powder. Crystals of **6** are obtained by layering a thf solution under hexane.

Yield: 0.063g (0,054 mmol, 22%)

Analytical data of **6**:

NMR (CD_2Cl_2 , 298 K)	^1H : δ [ppm] = 1.37 (s, 9H, $-(\text{C}_4\text{H}_9)$), 1.46 (s, 9H, $-(\text{C}_4\text{H}_9)$), 1.49 (s, 9H, $-(\text{C}_4\text{H}_9)$), 1.5 (very broad, $\omega_{1/2} \approx 80$ Hz, 18H, $-(\text{C}_4\text{H}_9)_2$), 1.52 (s, 9H, $-(\text{C}_4\text{H}_9)$), 1.79 (s, 15H, $-(\text{C}_5(\text{CH}_3)_5)$), 5.1 (very broad, $\omega_{1/2} \approx 80$ Hz, 2H, $\text{C}_5\text{H}_2^t\text{Bu}_3$) 5.16 (m broad, 1H, $\text{C}_5\text{H}_2^t\text{Bu}_3$), 5.20 (m broad, 1H, $\text{C}_5\text{H}_2^t\text{Bu}_3$). $^{31}\text{P}\{^1\text{H}\}$: two isomers present in solution Isomer 1: δ [ppm] = 126.0 (m, 1P), 144.1 (m, 1P), 465.5 (m, 1P), 501.1 (m, 1P). Isomer 2: δ [ppm] = 126.5 (m, 1P), 145.2 (m, 1P), 457.0 (m, 1P), 500.9 (m, 1P). Coupling constants of the cation are summarized in Table S7.
IR (CH_2Cl_2)	$\tilde{\nu}$ [cm^{-1}] = 1957 (m), 1985 (s), 2026 (s)
Elemental analysis ($\text{C}_{47}\text{H}_{73}\text{F}_6\text{Fe}_2\text{O}_3\text{P}_5\text{Ru}_1$)	Calculated: C 48.34, H 6.30 Found: C 45.18, H 5.77. The large deviation is probably caused by excess $[\text{Cp}^*\text{Ru}(\text{solv})_x][\text{PF}_6]$, which adsorbs on crystals of 6 . Due to its similar solubility to 6 , it cannot be removed by washing.
Mass spectrometry (ESI, CH_3CN)	m/z: 1023.2 (100%) [M] ⁺

2. Crystallographic Details

General remarks:

Single crystal structure analyses were performed using either Rigaku (formerly Agilent Technologies) diffractometer GV50, TitanS2 diffractometer (**6**) or a Gemini Ultra diffractometer (Oxford diffraction) with an AtlasS2 detector (**2, 3, 4**). Frames integration and data reduction were performed with the CrysAlisPro^[3] software package. All structures were solved either by ShelXT^[4] (**2, 3, 4**) or ShelXS^[5] (**6**) using the software Olex2^[6] and refined by full-matrix least-squares method against F^2 in anisotropic approximation using ShelXL.^[4] Hydrogen atoms were refined in calculated positions using riding on pivot atom model. Further details are given in Table S1.

CCDC-2051733 (**2**), CCDC-2051734 (**3**), CCDC-2051735 (**4**), and CCDC-2051736 (**6**) contain the supplementary crystallographic data for this paper. These data can be obtained free of charge at www.ccdc.cam.ac.uk/conts/retrieving.html (or from the Cambridge Crystallographic Data Centre, 12 Union Road, Cambridge CB2 1EZ, UK; Fax: + 44-1223-336-033; e-mail: deposit@ccdc.cam.ac.uk).

Table S1. Crystallographic data and details of diffraction experiments for **2, 3, 4**, and **6**.

Compound	2	3 · 2(CH ₂ Cl ₂)	4 · 2(CH ₂ Cl ₂)	6 · 0.7(C ₄ H ₈ O)
Formula	C ₄₈ H ₇₂ F ₁₂ Fe ₂ O ₄ P ₆ Ru	C ₅₀ H ₇₇ Cl ₄ F ₁₂ Fe ₂ O ₄ P ₆ Rh	C ₅₀ H ₇₇ Cl ₄ F ₁₂ Fe ₂ Ir O ₄ P ₆	C _{49.8} H _{78.6} F ₆ Fe ₂ O _{3.7} P ₅ Ru
$D_{calc}/g\text{ cm}^{-3}$	1.520	1.555	1.648	1.347
μ/mm^{-1}	0.986	9.179	2.890	7.558
Formula Weight	1339.64	1512.34	1601.63	1218.14
Color	clear dark yellow	clear orange	clear orange	dark red
Shape	plate	block	block	plate
Size/mm ³	0.46×0.31×0.25	0.17×0.13×0.09	0.38×0.25×0.12	0.32×0.16×0.11
T/K	123(1)	123(1)	123(1)	123.(1)
Crystal System	monoclinic	triclinic	triclinic	monoclinic
Space Group	$P2_1/n$	$P-1$	$P-1$	$P2_1/c$
$a/\text{Å}$	10.0919(2)	12.9624(4)	12.9537(2)	18.66252(20)
$b/\text{Å}$	14.4515(2)	14.8814(4)	14.8742(2)	16.39571(14)
$c/\text{Å}$	40.1739(6)	18.4164(4)	18.4134(2)	20.2876(3)
α°	90	73.521(2)	73.4890(10)	90
β°	92.7650(10)	72.266(3)	72.3460(10)	104.5480(11)
γ°	90	80.180(2)	80.0700(10)	90
$V/\text{Å}^3$	5852.26(17)	3230.90(16)	3226.85(8)	6008.68(11)
Z	4	2	2	4
Z'	1	1	1	1
Wavelength/Å	0.71073	1.54184	0.71073	1.54184
Radiation type	MoK _α	Cu K _α	Mo K _α	Cu K _α
Θ_{min}°	3.357	3.527	3.208	2.446
Θ_{max}°	32.463	71.928	32.890	74.387
Measured Refl's.	79434	34376	124329	63495
Ind't Refl's	19438	12257	22599	12096
Refl's with $I > 2(I)$	16675	11123	20785	11464
R_{int}	0.0374	0.0322	0.0305	0.0421
Parameters	744	825	772	645
Restraints	297	54	92	0
Largest Peak	0.688	0.519	1.068	0.622
Deepest Hole	-0.874	-0.554	-0.862	-0.982
GooF	1.080	1.014	1.028	1.042
wR_2 (all data)	0.0924	0.0671	0.0519	0.0887
wR_2	0.0880	0.0648	0.0503	0.0873
R_1 (all data)	0.0481	0.0328	0.0267	0.0349
R_1	0.0386	0.0283	0.0222	0.0332

X-ray diffraction on Crystals of 2

In the crystal structure of $[\{\text{Cp}^{\text{III}}\text{Fe}(\text{CO})_2\}_2(\mu_3, \eta^{4:1:1}\text{-P}_4)\{\text{CymRu}\}][\text{PF}_6]_2$ (**2**) a methyl group of the cymene ligand as well as one PF_6 anion is disordered over two positions and was refined to an occupancy of 56.459:43.541 and 65.893:34.107, respectively.

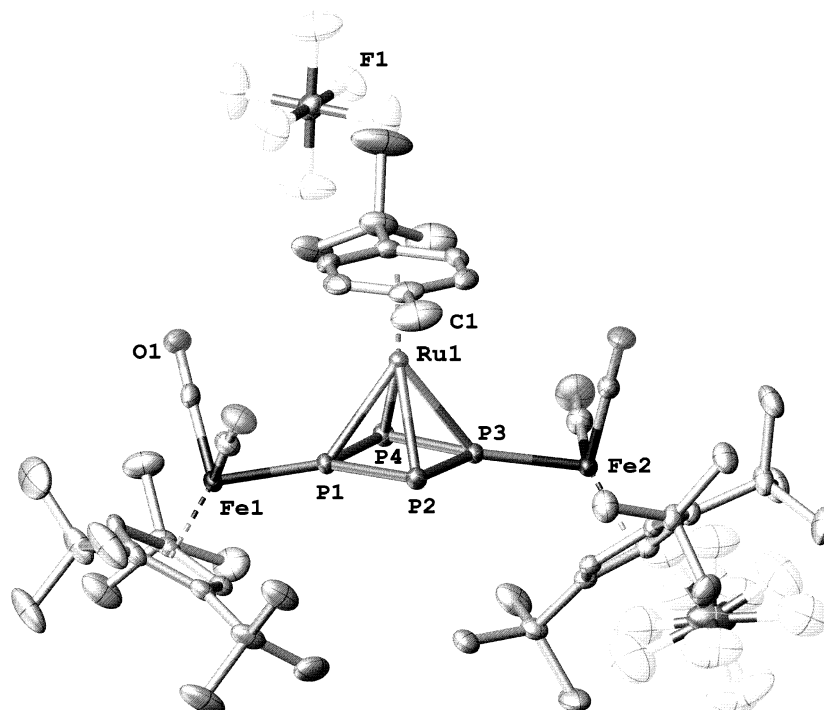


Figure S1. Molecular structure of **2** in the crystal. Hydrogen atoms are omitted for clarity. ADPs are drawn at 50% probability level. Selected bond length [Å] and angles [°] are: P1-P4 2.1410(7), P1-P2 2.1434(7), P4-P3 2.1481(7), P3-P2 2.1356(7), Fe1-P1 2.1800(5), Fe2-P3 2.1813(5), Ru1-P_{4,cent.} 1.8890(2), Ru1-C_{6,cent.} 1.7433(8), P4-P1-P2 97.34(3), P1-P4-P3 82.50(2), P2-P3-P4 97.37(3), P3-P2-P1 82.74(2).

X-ray diffraction on Crystals of 3

In the crystal structure of $[\{\text{Cp}^{\text{III}}\text{Fe}(\text{CO})_2\}_2(\mu_3, \eta^{4:1:1}\text{-P}_4)\{\text{Cp}^*\text{Rh}\}][\text{PF}_6]_2 \cdot 2(\text{CH}_2\text{Cl}_2)$ (**3**) the two CH_2Cl_2 molecules as well as one PF_6 anion is disordered over two positions and was refined to an occupancy of 70:30, 55:45 and 90:10, respectively.

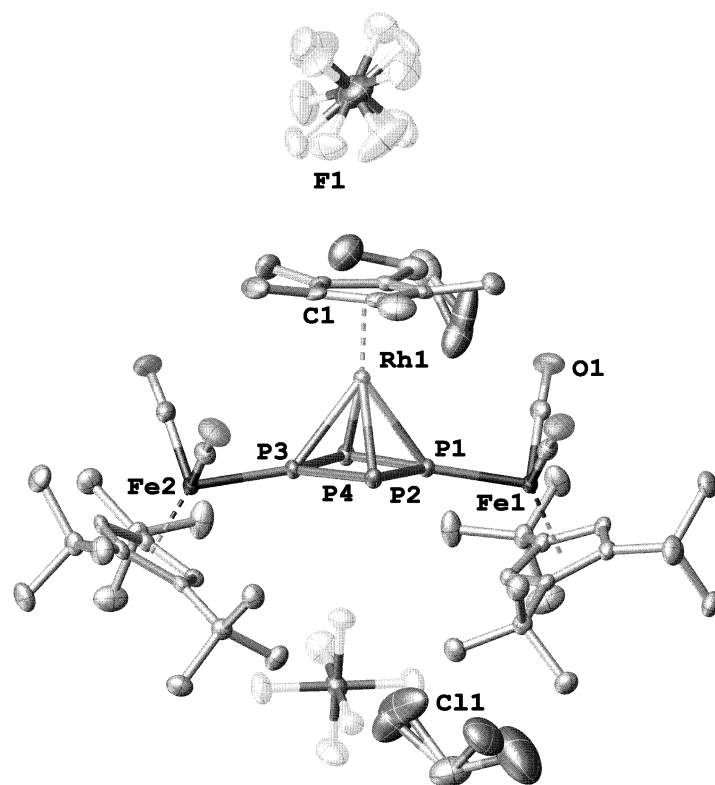


Figure S2. Molecular structure of **3** in the crystal. Hydrogen atoms are omitted for clarity. ADPs are drawn at 50% probability level. Selected bond length [Å] and angles [°] are: P1-P4 2.1456(8), P1-P2 2.1447(8), P4-P3 2.1459(8), P3-P2 2.1433(8), Fe1-P1 2.2100(6), Fe2-P3 2.2091(6), Rh1-P_{4,cent.} 1.8938(3), Rh1-Cp*_{cent.} 1.8531(10), P4-P1-P2 97.34(3), P1-P4-P3 83.02(3), P2-P3-P4 96.91(3), P3-P2-P1 83.10(3).

X-ray diffraction on Crystals of 4

In the crystal structure of $[\{\text{Cp}^{\text{III}}\text{Fe}(\text{CO})_2\}_2(\mu_3, \eta^{4:1:1}\text{-P}_4)\{\text{Cp}^*\text{Ir}\}][\text{PF}_6]_2 \cdot 2(\text{CH}_2\text{Cl}_2)$ (**4**) a chlorine atom of a CH_2Cl_2 molecule as well as the second CH_2Cl_2 molecule is disordered over two positions and was refined to an occupancy of 60:40 and 70.563:29.437, respectively.

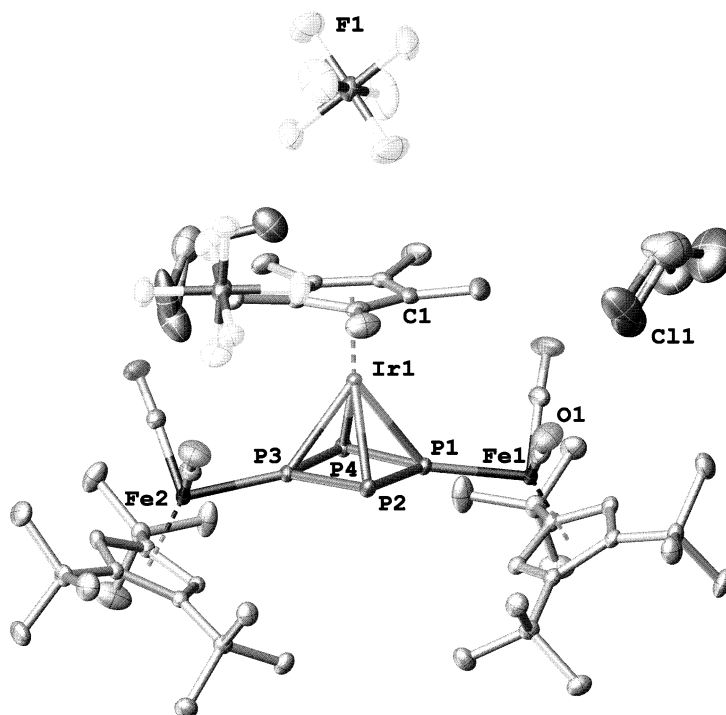


Figure S3. Molecular structure of **4** in the crystal. Hydrogen atoms are omitted for clarity. ADPs are drawn at 50% probability level. Selected bond length [Å] and angles [°] are: P1-P4 2.1488(6), P1-P2 2.1512(6), P4-P3 2.1501(6), P3-P2 2.1518(6), Fe1-P1 2.2073(4), Fe2-P3 2.2074(4), Ir1-P_{4,cent.} 1.8915(2), Ir1-Cp*_{cent.} 1.8542(7), P4-P1-P2 96.82(2), P1-P4-P3 83.10(2), P2-P3-P4 96.76(2), P3-P2-P1 83.20(2).

X-ray diffraction on Crystals of 6

In the crystal structure of $[\{\text{Cp}^{\text{III}}\text{Fe}(\text{CO})_2\}\{\text{Cp}^{\text{III}}\text{Fe}(\text{CO})\}(\mu_3, \eta^{4:2:1}\text{-P}_4)(\text{Cp}^*\text{Ru})][\text{PF}_6] \cdot 0.7(\text{C}_4\text{H}_8\text{O})$ (**6**) only one of the two enantiomers (Figure S4: 1S-2R-3R-4R-5S enantiomer, Figure S5: 1R-2S-3S-4S-5R enantiomer) is present in the asymmetric unit. The second enantiomer is obtained by symmetry generation. The position of thf molecule is occupied by 70%.

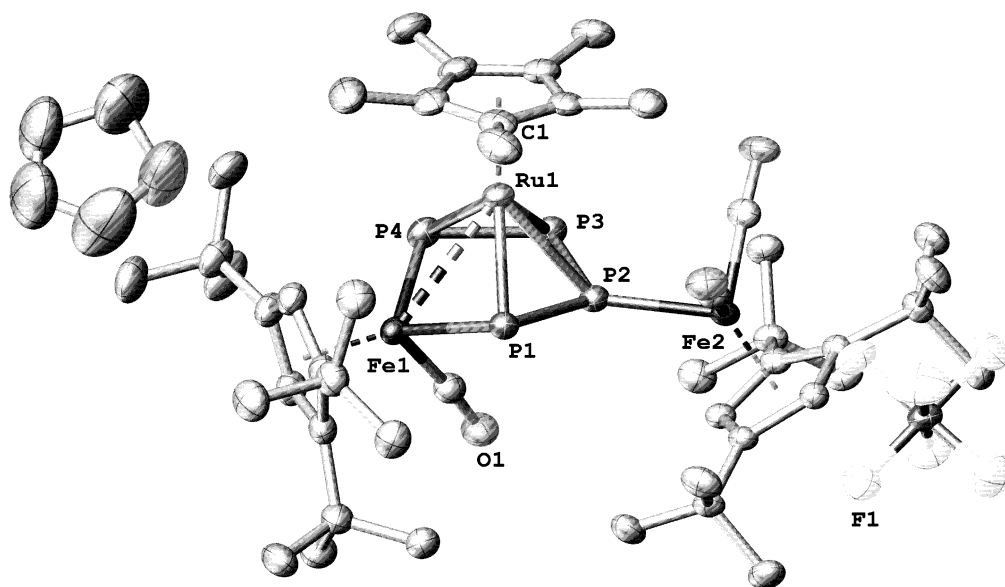


Figure S4. Molecular structure of the 1S-2R-3R-4R-5S enantiomer of **6** in the crystal. Hydrogen atoms are omitted for clarity. ADPs are drawn at 50% probability level. Selected bond length [\AA] and angles [$^\circ$] are: P1-P2 2.1360(8), P2-P3 2.1335(8), P3-P4 2.1446(8), Ru1-P1 2.3592(5), Ru1-P2 2.4454(5), Ru1-P3 2.4469(6), Ru1-P4 2.3513(6), Ru1 \cdots Fe1 2.9052(4), Fe1-P1 2.2539(6), Fe1-P4 2.2498(7), Fe2-P2 2.2413(6), Ru1-Cp*_{cent.} 1.9069(10), P4-Fe1-P1 99.44(2), P2-P1-Fe1 102.26(3), P3-P2-P1 111.67(3), P3-P4-Fe1 108.53(3).

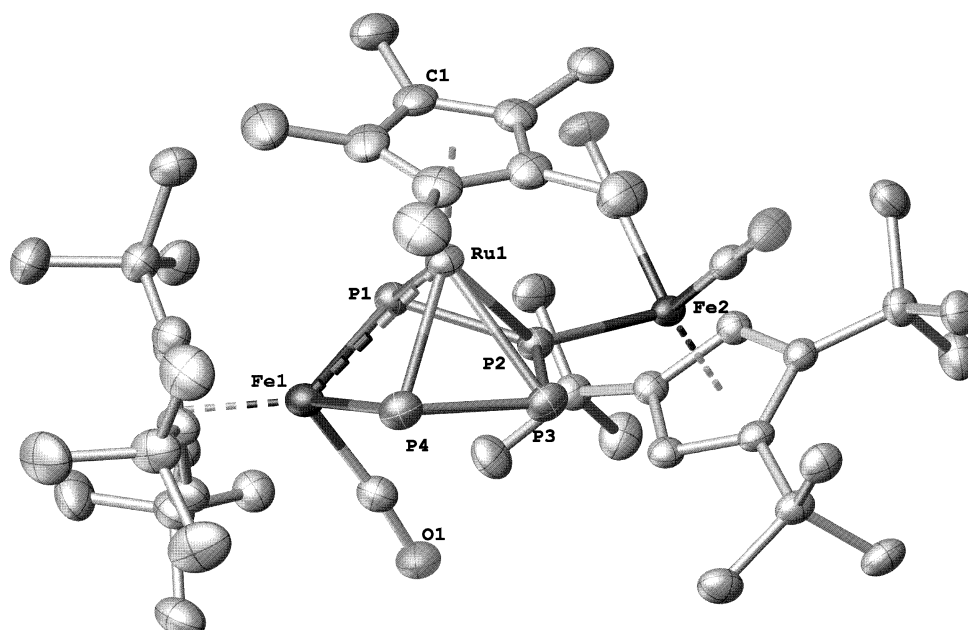
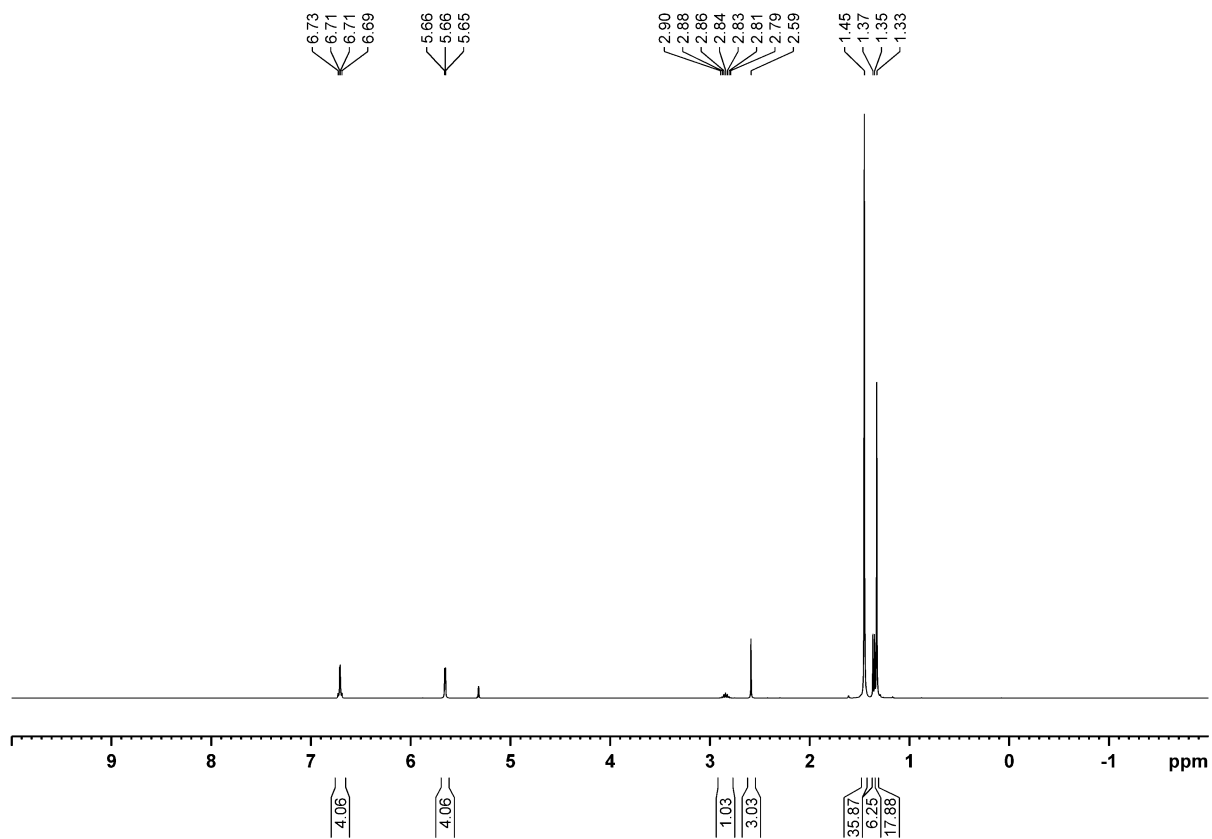


Figure S5. Molecular structure of the cationic part of the 1R-2S-3S-4S-5R enantiomer of **6** in the crystal. Hydrogen atoms are omitted for clarity. ADPs are drawn at 50% probability level.

3. ^1H NMR and ^{31}P NMR Spectroscopy

General remarks:

^1H and ^{31}P NMR spectra were recorded on a Bruker Avance III HD 400 (^1H : 400.130 MHz, ^{31}P : 161.976 MHz) at 298 K. The chemical shifts are reported in ppm relative to external TMS (^1H) and H_3PO_4 (^{31}P). The ^{31}P NMR simulation was performed with the simulation tool of Bruker TopSpin (Version 4.0.8.).



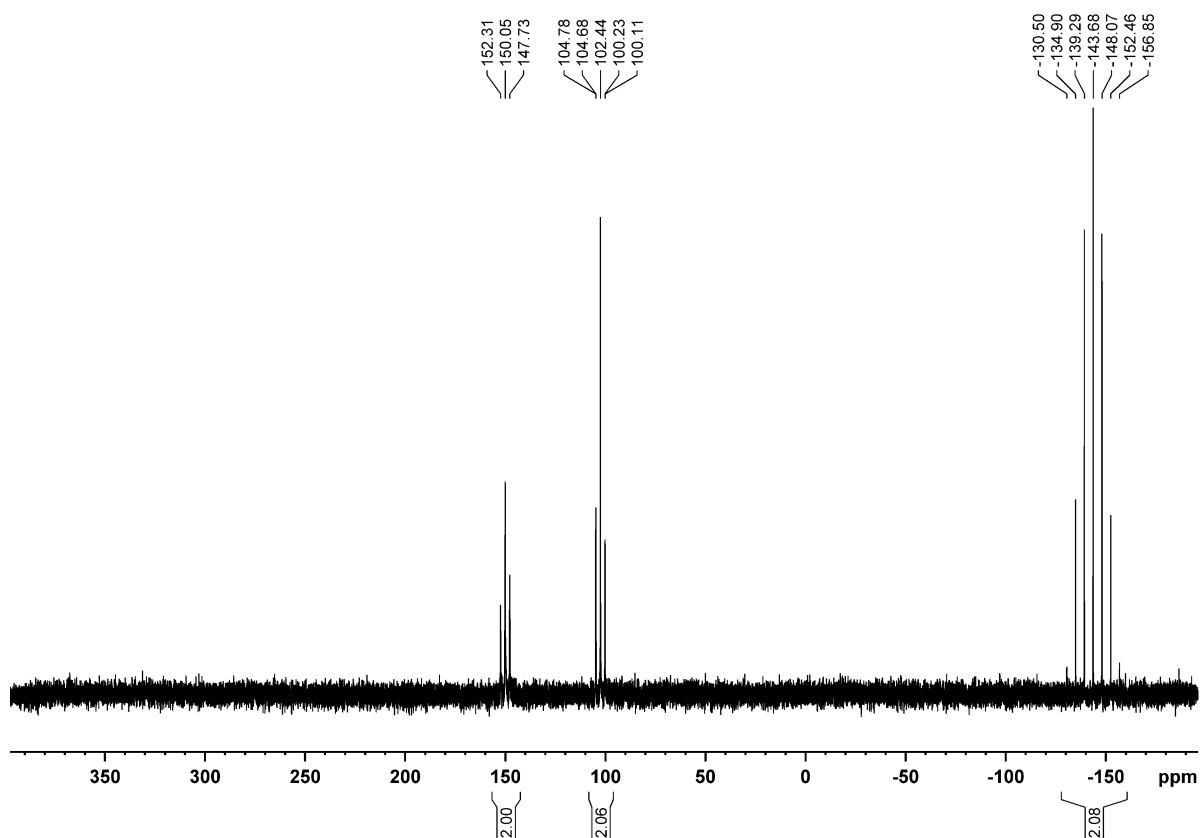


Figure S7. $^{31}\text{P}\{^1\text{H}\}$ NMR spectrum of **2** in CD_2Cl_2 .

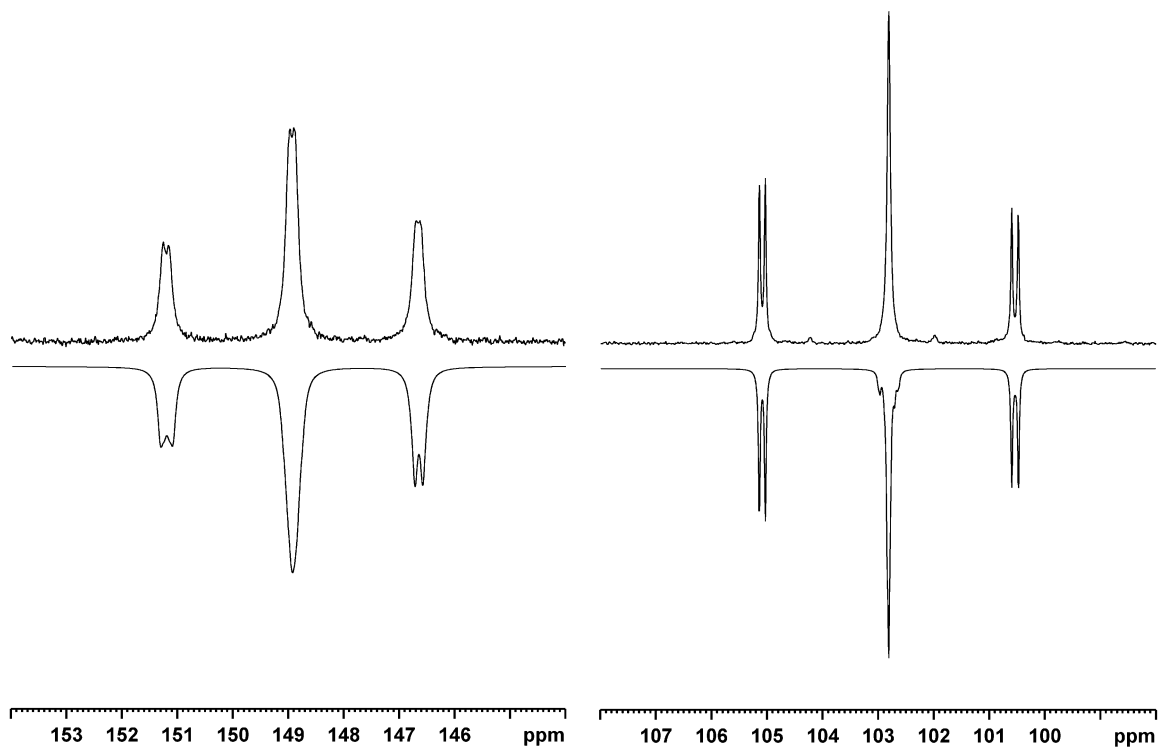


Figure S8. Experimental (top) and simulated (bottom) $^{31}\text{P}\{^1\text{H}\}$ NMR spectrum of **2** ($\text{AA}'\text{XX}'$ spin system).

Table S2. Calculated coupling constants of the cation of **2** (AA'XX' spin system) with a R-factor of 1.66%.

Chemical shift [ppm]		Coupling constants [Hz]			
A	148.9	J_{AX}	377.3	$J_{AA'}$	13.8
A'	148.8	$J_{AX'}$	366.5	$J_{XX'}$	14.4
X	102.9	$J_{A'X}$	362.3		
X'	102.9	$J_{A'X'}$	369.2		

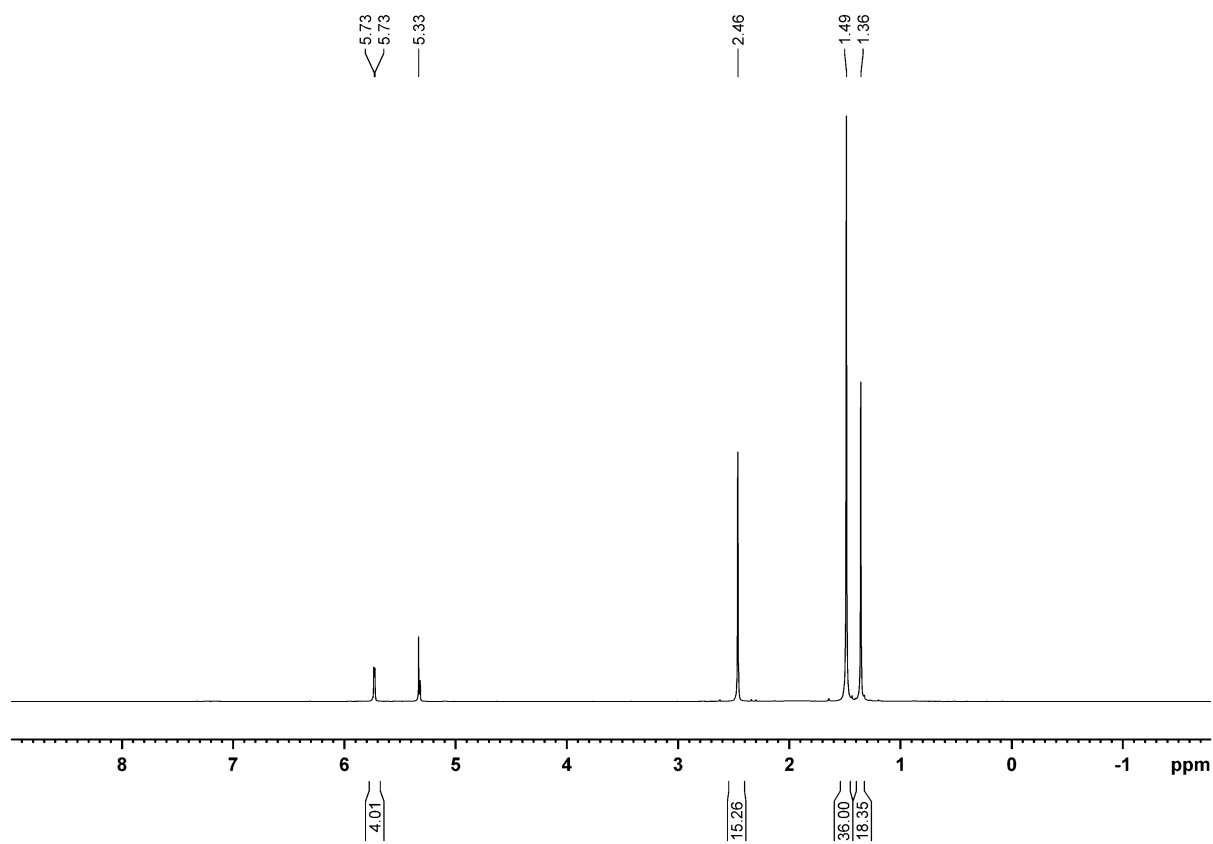
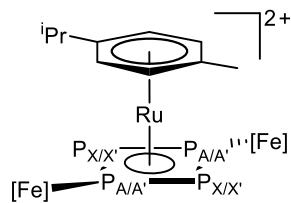


Figure S9. ^1H NMR spectrum of **3** in CD_2Cl_2 .

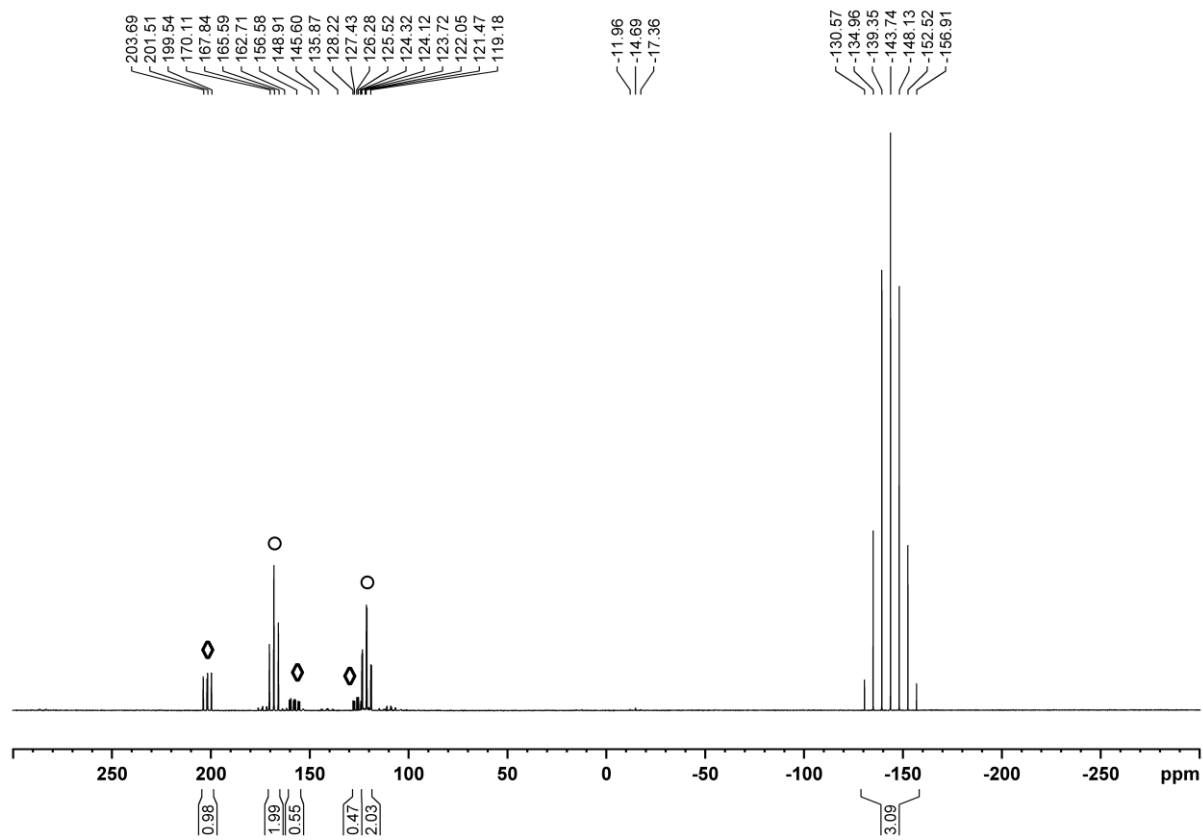


Figure S10. $^{31}\text{P}\{^1\text{H}\}$ NMR spectrum of the reaction solution of **3** in CD_2Cl_2 . The signals marked with a circle (\circ) can be assigned to **3**, while the signals marked with a diamond (\diamond) indicate the formation of a side products with an AA'MNX spin system (see Figure S13, Table S4 and Scheme S1).

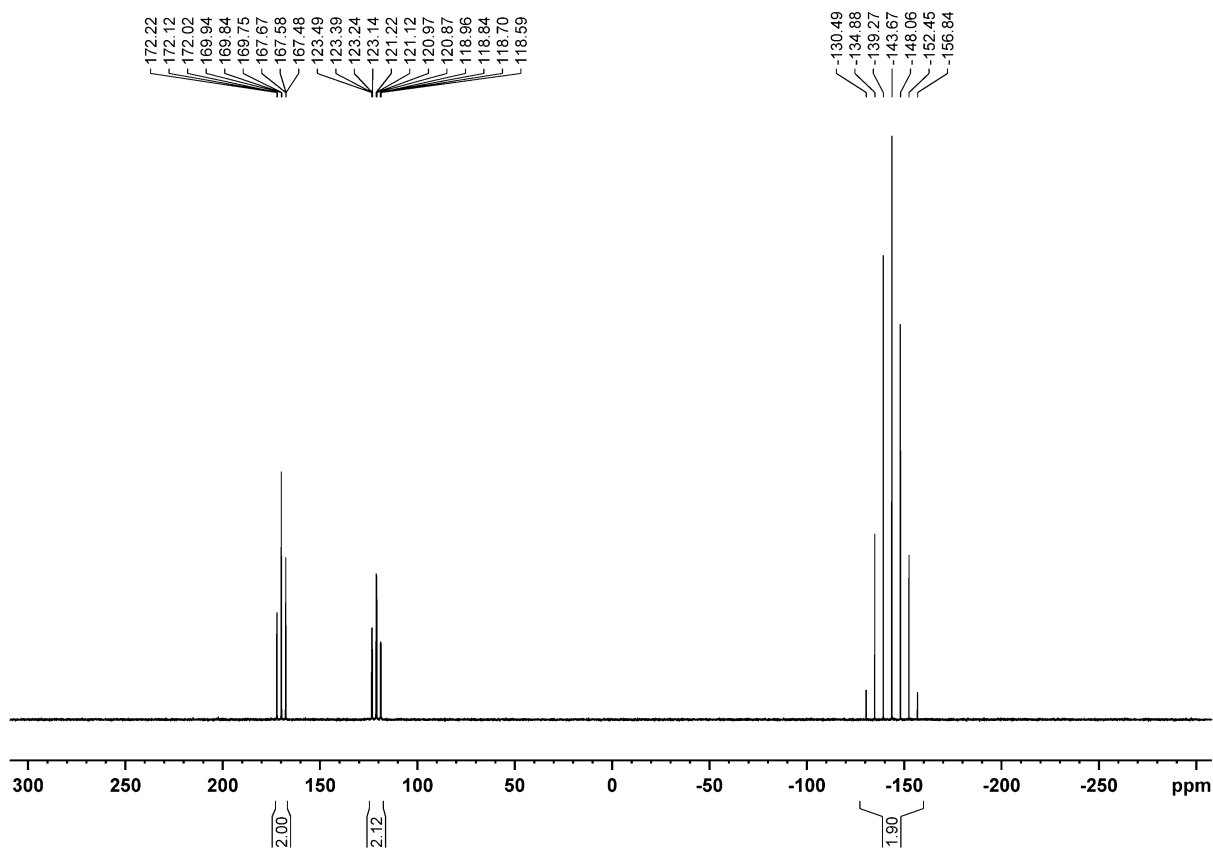


Figure S11. $^{31}\text{P}\{^1\text{H}\}$ NMR spectrum of **3** in CD_2Cl_2 .

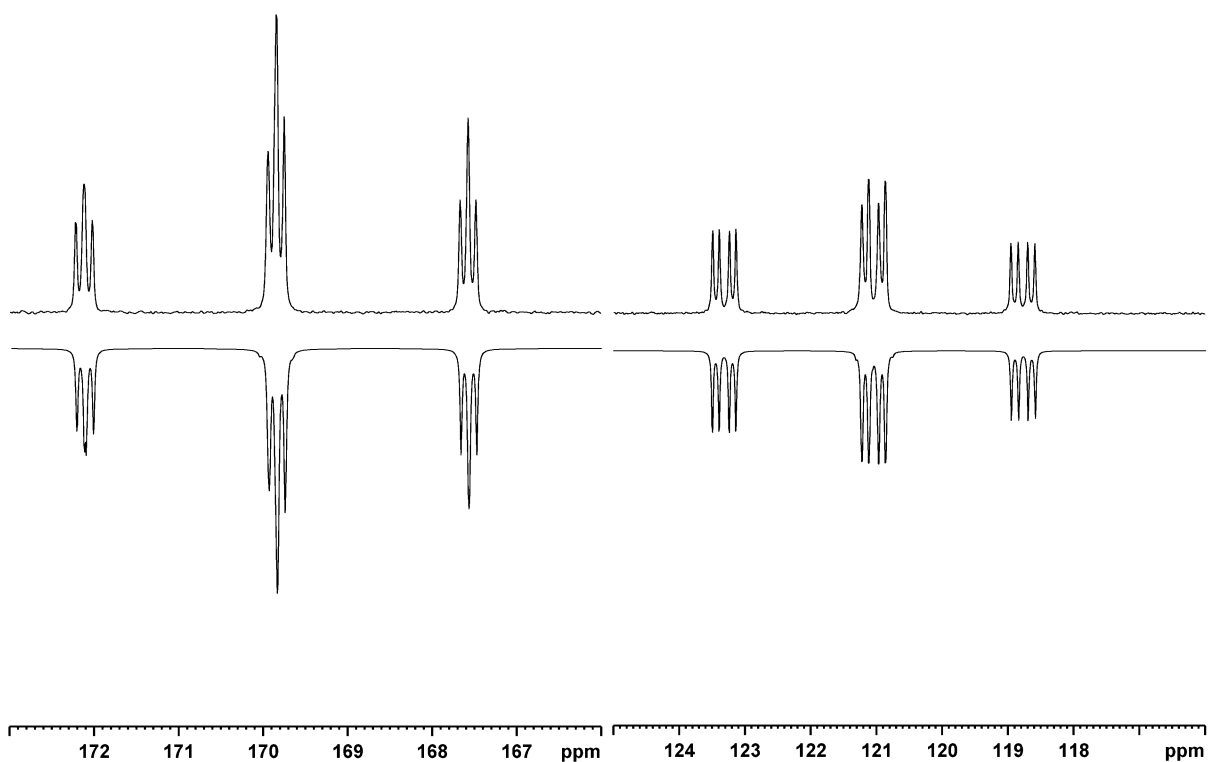
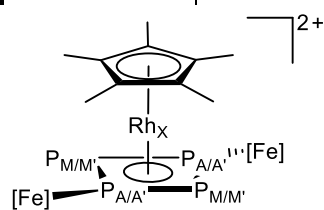


Figure S12. Experimental (top) and simulated (bottom) $^{31}\text{P}\{^1\text{H}\}$ NMR spectrum of **3** (AA'MM'X spin system, X corresponds to Rh).

Table S3. Calculated coupling constants of the cation of **3** (AA'MM'X spin system) with a R-factor of 1.15%.

Chemical shift [ppm]		Coupling constants [Hz]					
A	169.8	J_{AM}	372.7	$J_{AA'}$	1.9	J_{MX}	41.0
A'	169.8	$J_{AM'}$	364.4	$J_{MM'}$	15.3	$J_{M'X}$	41.4
M	121.1	$J_{A'M}$	365.1	J_{AX}	13.9		
M'	121.1	$J_{A'M'}$	370.8	$J_{A'X}$	13.7		



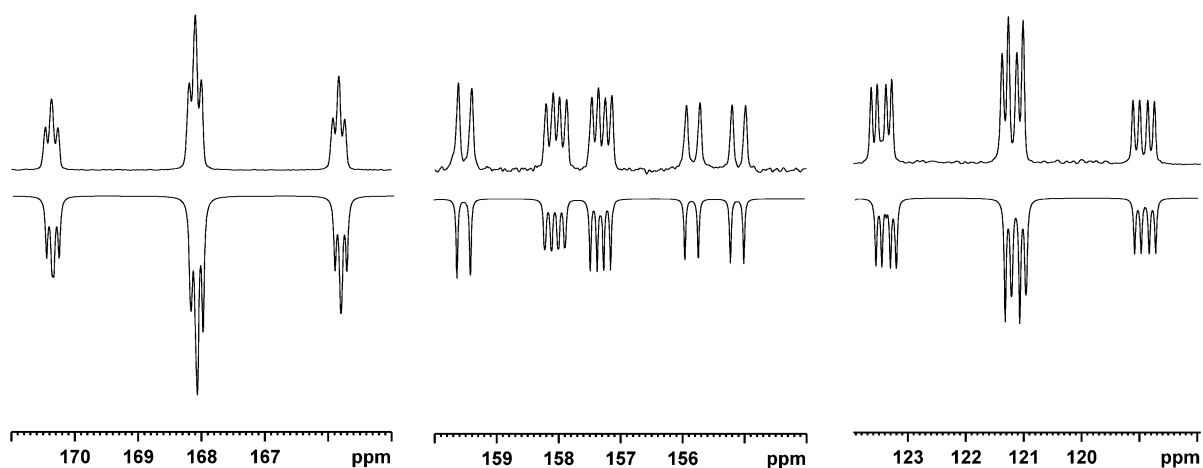
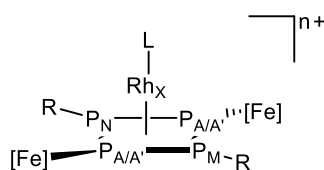


Figure S13. Experimental (top) and simulated (bottom) $^{31}\text{P}\{^1\text{H}\}$ NMR spectrum of the side product with an AA'MNX spin system (X corresponds to Rh) of the synthesis of **3** (see Figure S10).

Table S4. Calculated coupling constants of the side product in the synthesis of **3** (AA'MNX spin system) with a R-factor of 3.67%.

Chemical shift [ppm]		Coupling constants [Hz]					
A	201.7	J_{AM}	359.4	J_{NM}	118.8	J_{MX}	35.1
A'	201.7	J_{AN}	315.9	$J_{AA'}$	12.8	J_{NX}	24.8
M	157.7	$J_{A'M}$	356.8	J_{AX}	15.7		
N	125.7	$J_{A'N}$	314.7	$J_{A'X}$	15.7		



Scheme S1. Postulated structure of the byproduct based on the coupling constants obtained by the simulation. R and L are possible pattern for substitution.

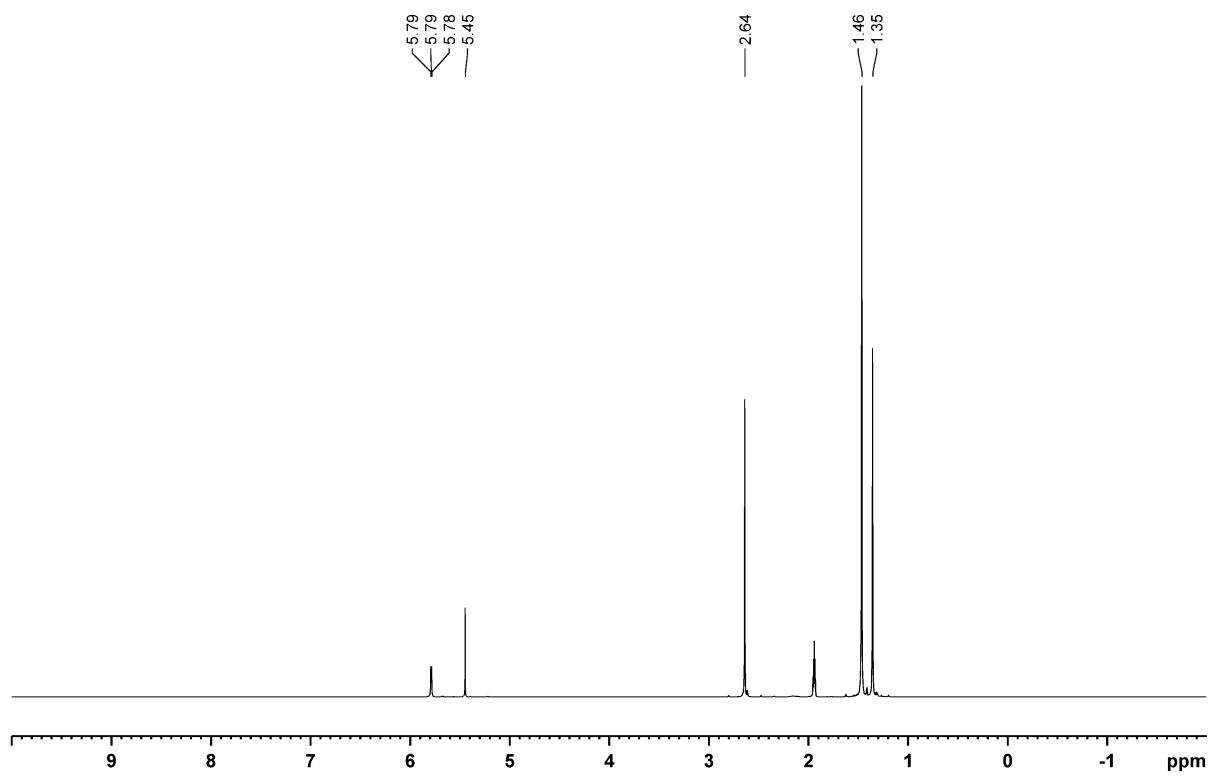


Figure S14. ^1H NMR spectrum of **4** in CD_3CN .

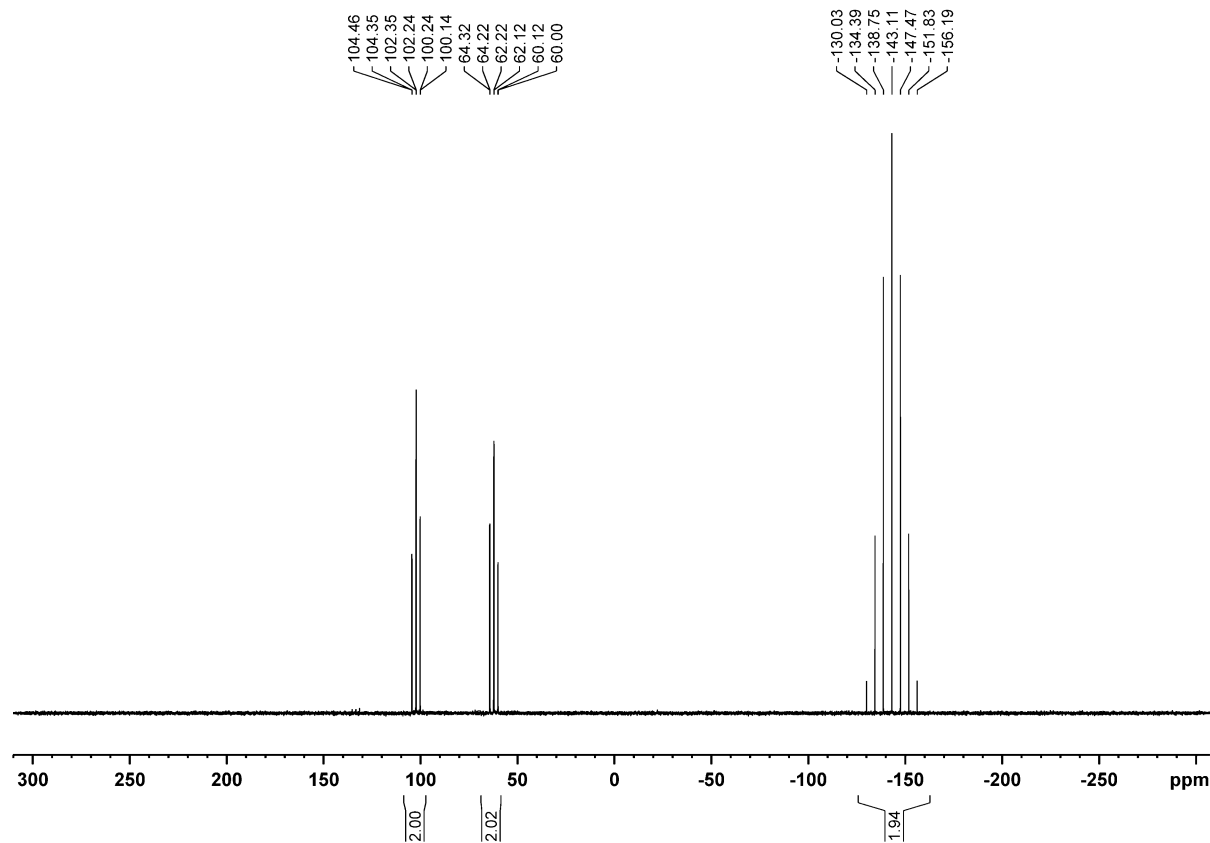


Figure S15. $^{31}\text{P}\{^1\text{H}\}$ NMR spectrum of **4** in CD_3CN .

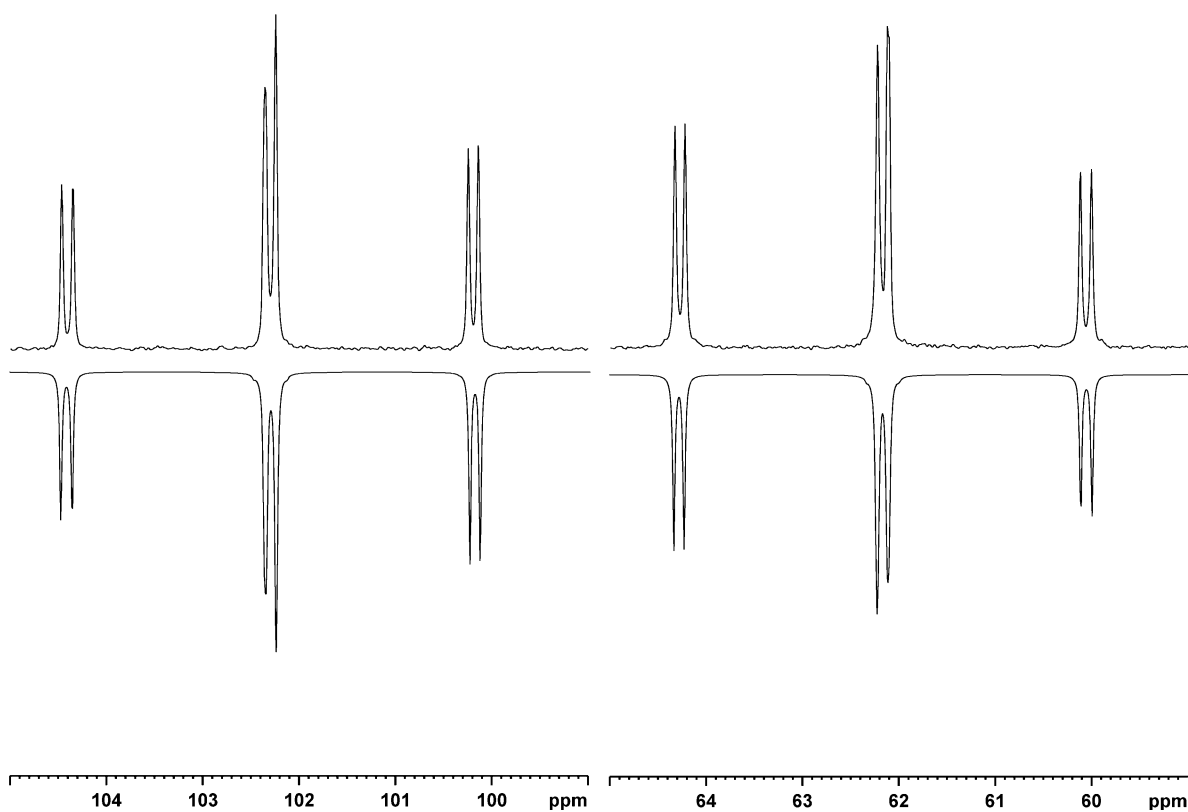
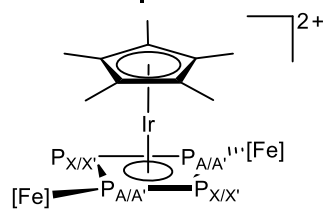


Figure S16. Experimental (top) and simulated (bottom) $^{31}\text{P}\{^1\text{H}\}$ NMR spectrum of **4** (AA'XX' spin system).

Table S5. Calculated coupling constants of the cation of **4** (AA'XX' spin system) with a R-factor of 1.08%.

Chemical shift [ppm]		Coupling constants [Hz]	
A	102.3	J_{AX}	338.1
A'	102.3	$J_{AX'}$	343.1
X	62.2	$J_{A'X}$	345.6
X'	26.2	$J_{A'X'}$	340.2
		$J_{AA'}$	17.9



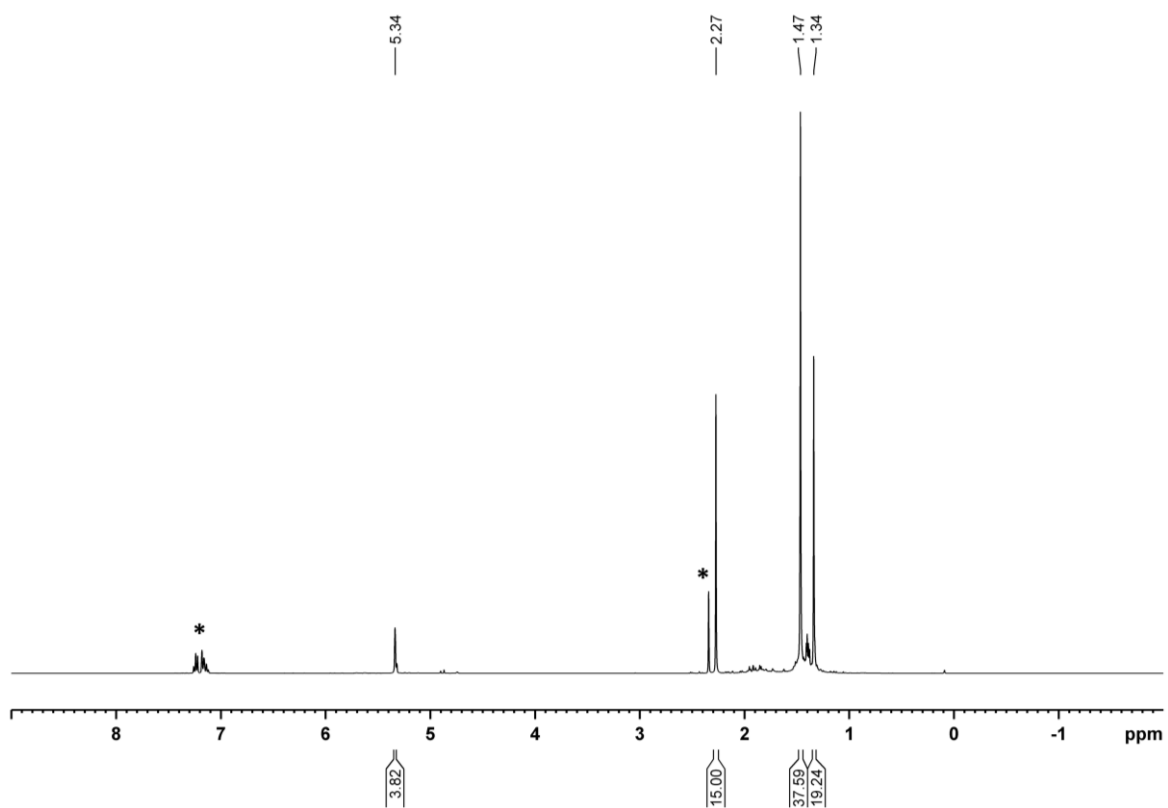


Figure S17. ^1H NMR spectrum of **5** in CD_2Cl_2 . Signals marked with a star (*) are assigned to toluene.

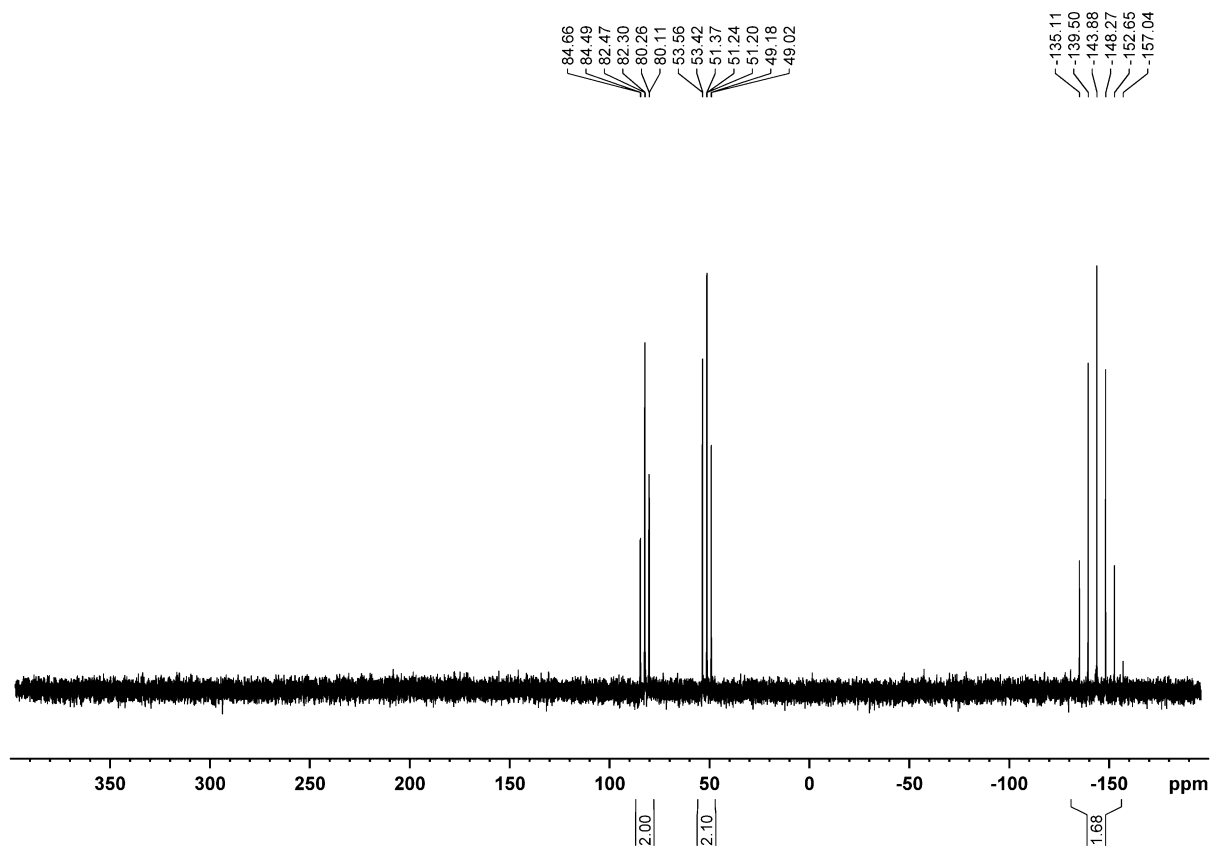


Figure S18. $^{31}\text{P}\{^1\text{H}\}$ NMR spectrum of **5** in CD_2Cl_2 .

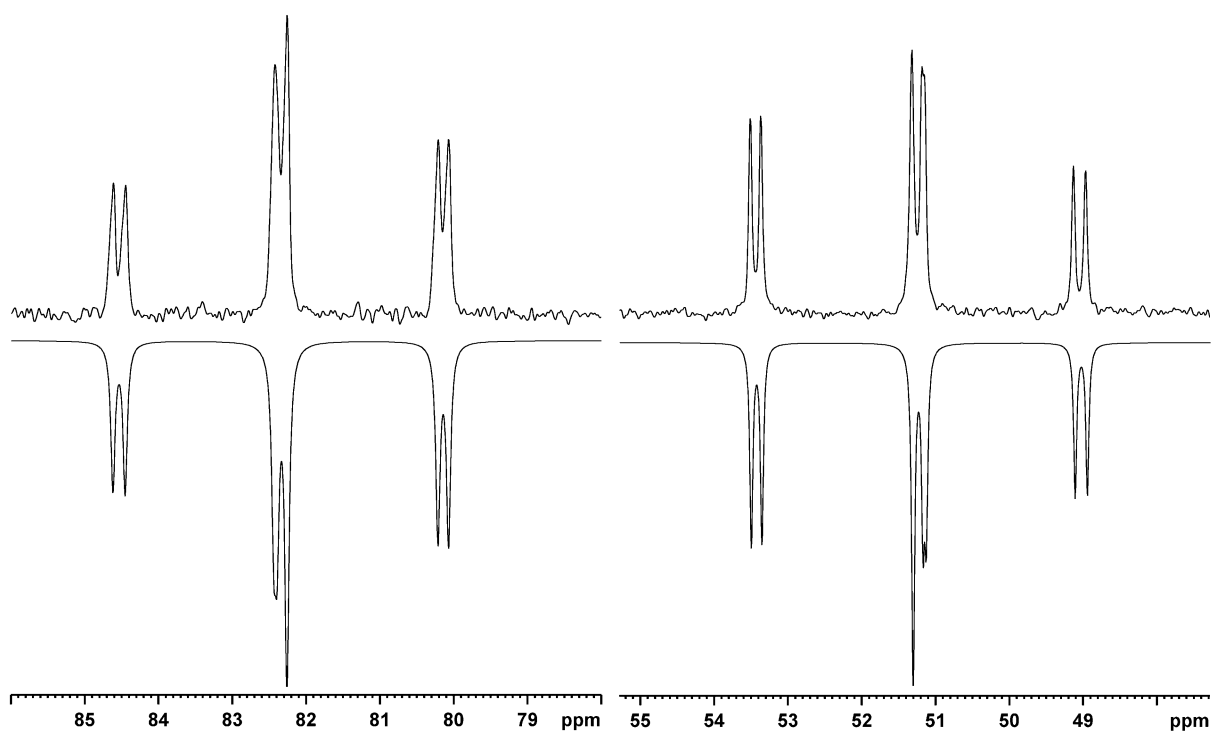
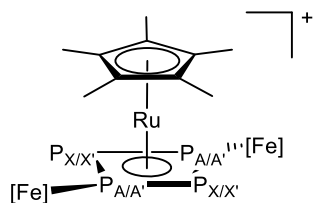


Figure S19. Experimental (top) and simulated (bottom) $^{31}\text{P}\{^1\text{H}\}$ NMR spectrum of **5** (AA'XX' spin system).

Table S6. Calculated coupling constants of the cation of **5** (AA'XX' spin system) with a R-factor of 2.74%.

	Chemical shift [ppm]	Coupling constants [Hz]			
A	82.0	J_{AX}	352.6	$J_{AA'}$	25.9
X	82.0	$J_{AX'}$	361.5	$J_{XX'}$	31.4
X	51.7	$J_{A'X}$	359.4		
X'	51.7	$J_{A'X'}$	352.3		



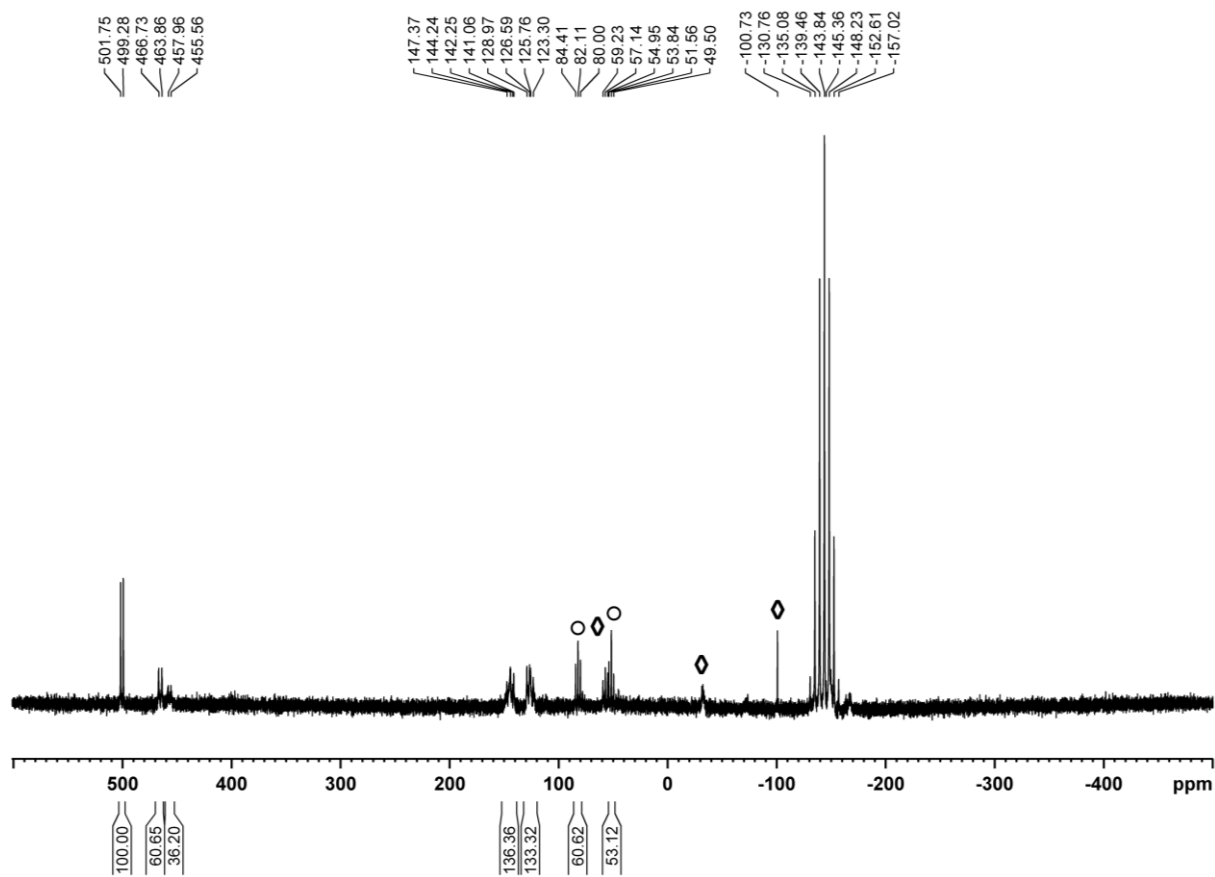


Figure S20. $^{31}\text{P}\{^1\text{H}\}$ NMR spectrum of the reaction mixture of **6** in CD_2Cl_2 . The signals marked with the circle (\circ) can be assigned to **5**, while the signals marked with a diamond (\diamond) indicate the formation of side or degradation products.

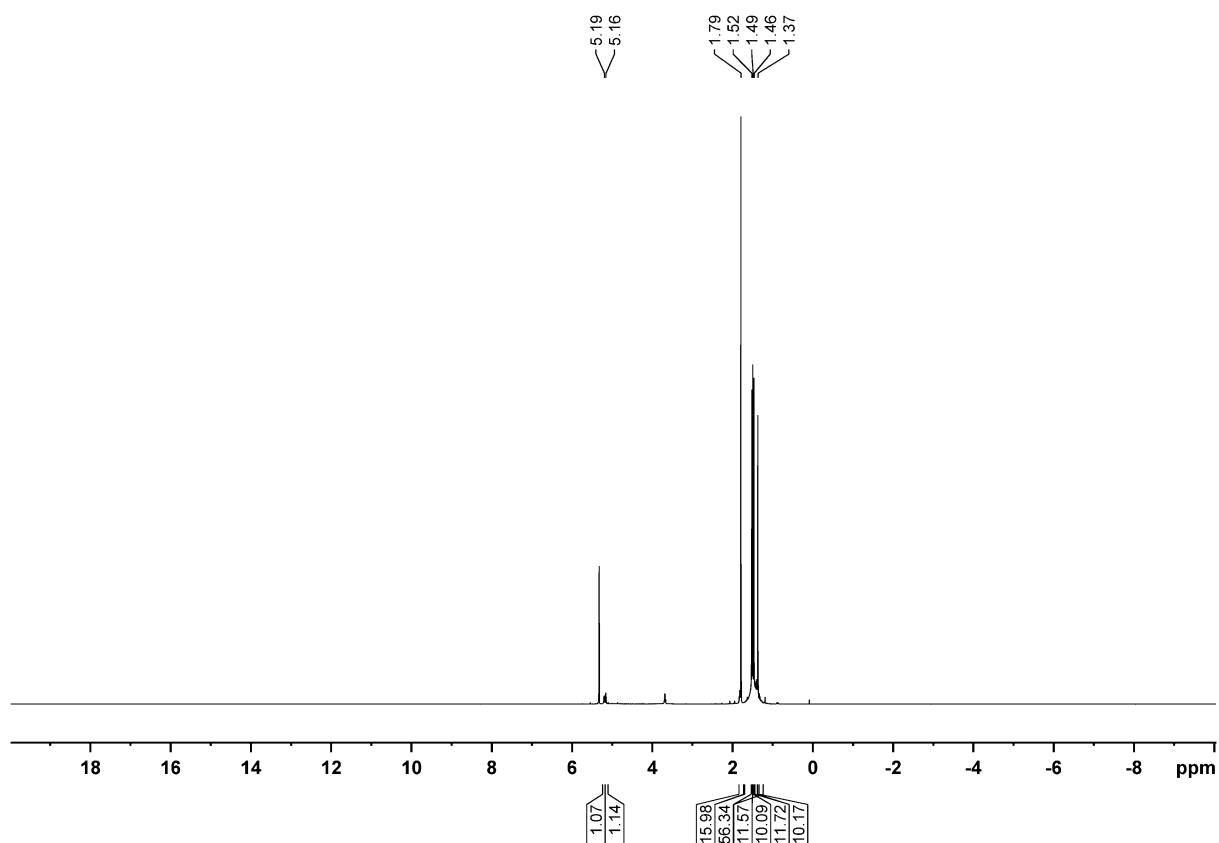


Figure S21. ^1H NMR spectrum a crystalline sample of **6** in CD_2Cl_2 . The aliphatic region (approx. $\delta = 1.3 - 1.7$ ppm) shows four singlets with an integral of approx. 9 each. Additionally, a broad signal lays underneath the four singlets with an integral of 18 ($56 - (4 \times 9) \approx 18$).

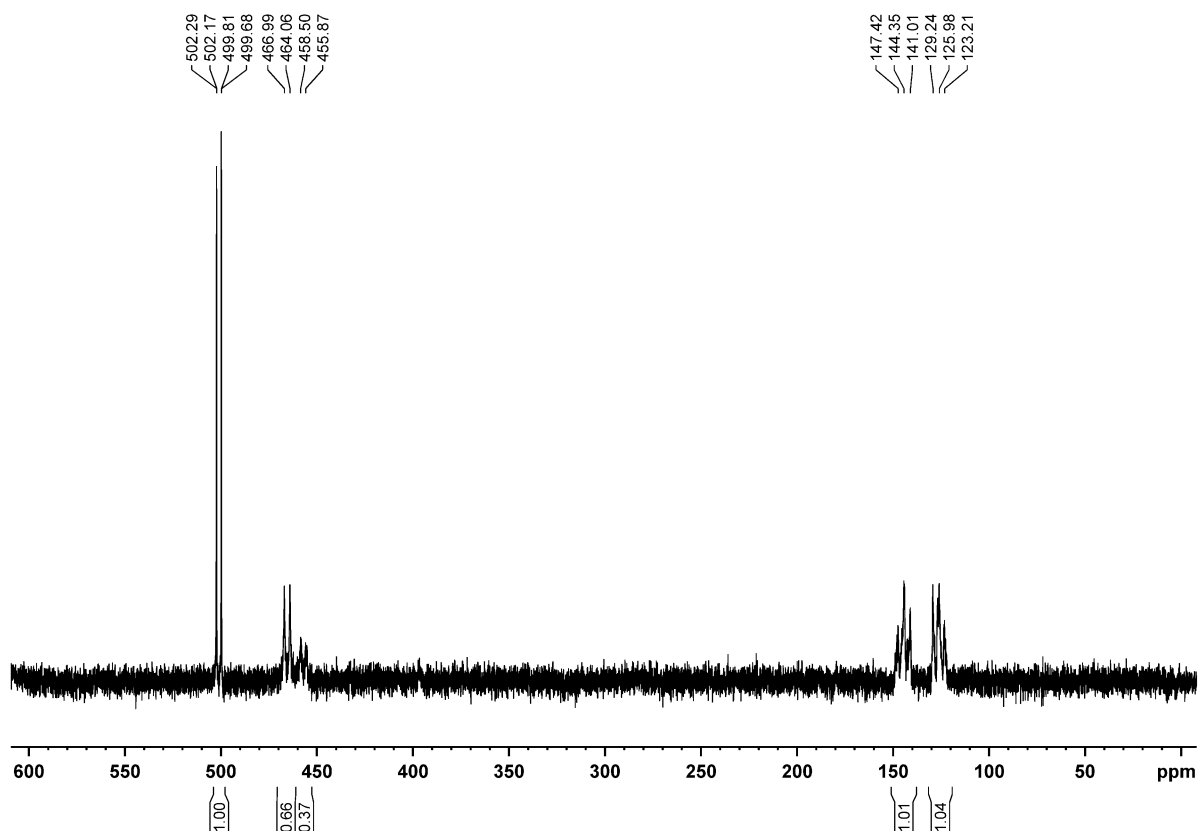


Figure S22. $^{31}\text{P}\{^1\text{H}\}$ NMR spectrum of a crystalline sample of **6** in CD_2Cl_2 that indicates the presence of two isomers in solution.

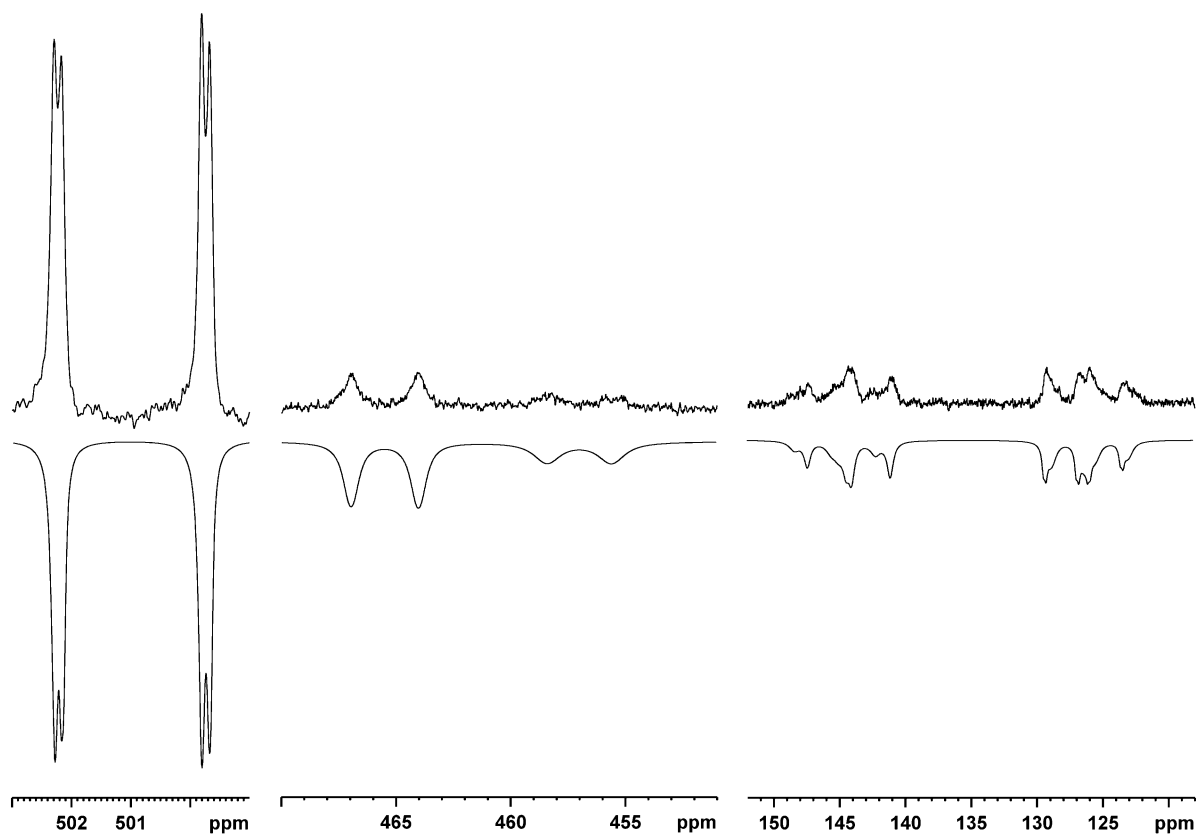
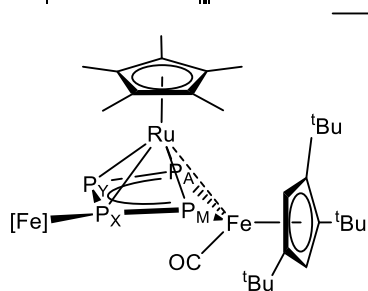


Figure S23. Experimental (top) and simulated (bottom) $^{31}\text{P}\{^1\text{H}\}$ NMR spectrum of **6** (AMXY spin system).

Table S7. Calculated coupling constants of the two isomers of **6** (AMXY spin system) with a R-factor of 1.76%. The two isomers were refined to a distribution of 63% to 37%.

Isomer 1				Isomer 2							
Chemical shift [ppm]		Coupling constants [Hz]		Chemical shift [ppm]		Coupling constants [Hz]					
A	501.1	J_{AY}	406.5	J_{AM}	3.2	A	500.9	J_{AY}	407.3	J_{AM}	6.8
M	465.5	J_{MX}	480.6	J_{AX}	-3.4	M	457.0	J_{MX}	458.0	J_{AX}	-8.6
X	144.1	J_{XY}	544.9	J_{MY}	26.7	X	145.2	J_{XY}	546.1	J_{MY}	30.1
Y	126.0					Y	126.5				



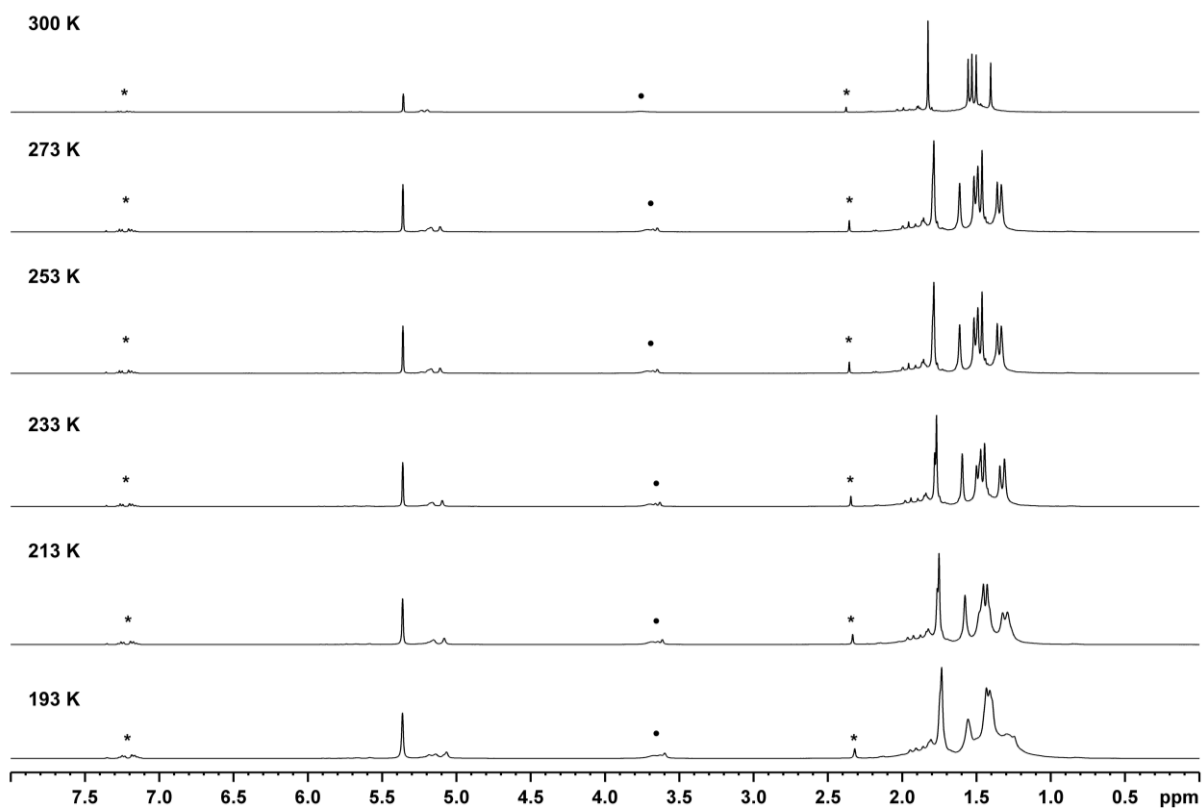


Figure S24. ^1H NMR spectra of a crystalline sample of **6** in CD_2Cl_2 at different temperatures. Signals marked with a star (*) are assigned to toluene, while the broad signals marked with a dot (•) are assigned to impurities of $[\text{Cp}^*\text{Ru}(\text{thf})_x][\text{PF}_6]$.

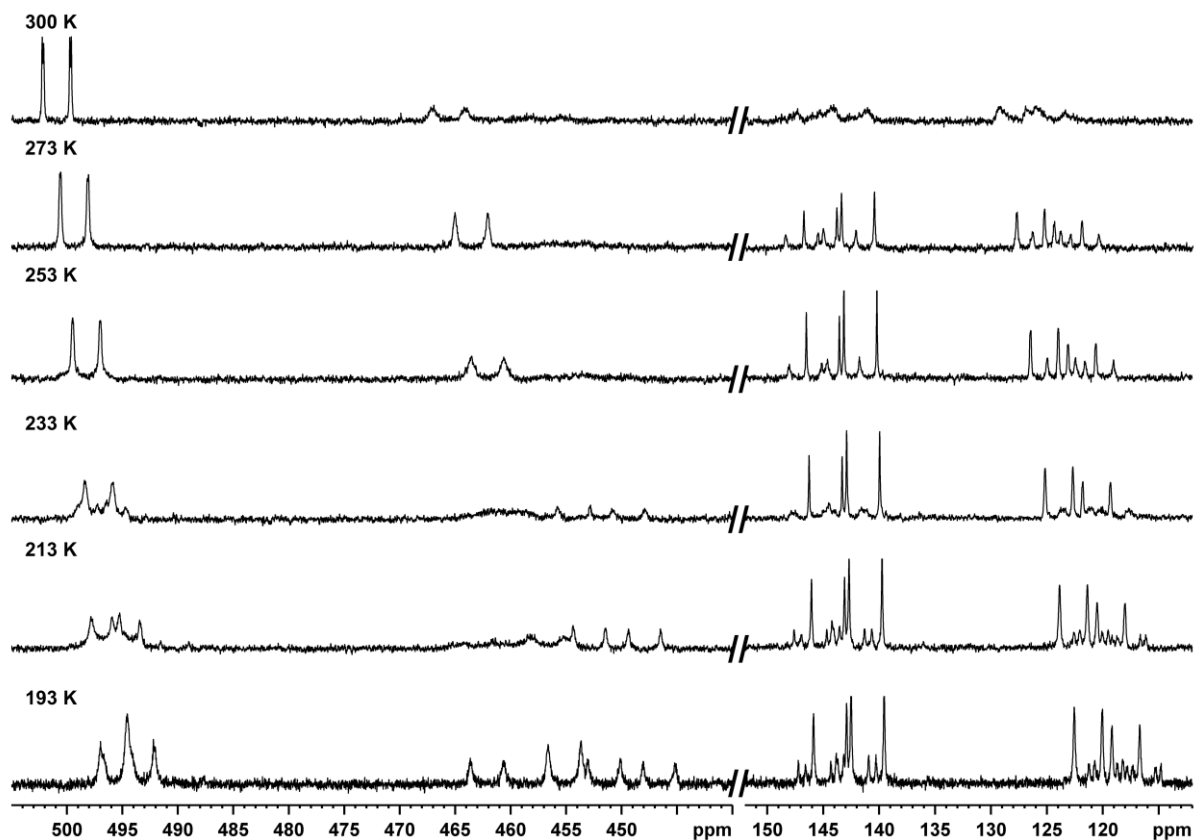


Figure S25. $^{31}\text{P}\{^1\text{H}\}$ NMR spectra of a crystalline sample of **6** in CD_2Cl_2 at different temperatures.

4. Computational Details

All calculations have been performed with the TURBOMOLE program package^[7] at the RI^[8,9]-BP86^[10]/def2-TZVP^[9,11] level of theory. To speed up the geometry optimization the Multipole Accelerated Resolution-of-the-Identity (MARI-J)^[8,9,12] approximation has been used. For the reaction energies single point calculations at the B3LYP/def2-TZVP level have been performed in which the solvent effects have been incorporated via the COSMO method (acetonitrile $\epsilon = 35.688$). The numbering of the atoms in the computational part differs from that of the main part.

Table S8. Partial charge of the fragments of **6**, **7**, **5** and **2**.

		Partial charge	Percentage [%]		Partial charge	Percentage [%]
Complex	6			7		
Iron fragment	Cp ^{'''} Fe ₂ (CO)	0.08	8.00	Cp ^{'''} Fe ₂ (CO)	0.33	16.39
Iron fragment	Cp ^{'''} Fe ₃ (CO) ₂	0.34	34.38	Cp ^{'''} Fe ₃ (CO) ₂	0.49	24.70
Ligand (Ru)	Cp*	0.29	28.74	Cym	0.64	32.17
Ruthenium	Ru1	-0.35	-35.00	Ru1	-0.40	-20.12
P ₄ unit	P ₄	0.64	63.88	P ₄	0.94	46.86
Total charge		1.00	100.00		2.00	100.00
Complex	5			2		
Iron fragment	Cp ^{'''} Fe ₂ (CO) ₂	0.35	35.22	Cp ^{'''} Fe ₂ (CO) ₂	0.51	25.73
Iron fragment	Cp ^{'''} Fe ₃ (CO) ₂	0.34	34.30	Cp ^{'''} Fe ₃ (CO) ₂	0.52	25.76
Ligand (Ru)	Cp*	0.18	18.04	Cym	0.52	26.01
Ruthenium	Ru1	-0.37	-37.04	Ru1	-0.41	-20.26
P ₄ unit	P ₄	0.49	49.48	P ₄	0.86	42.76
Total charge		1.00	100.00		2.00	100.00

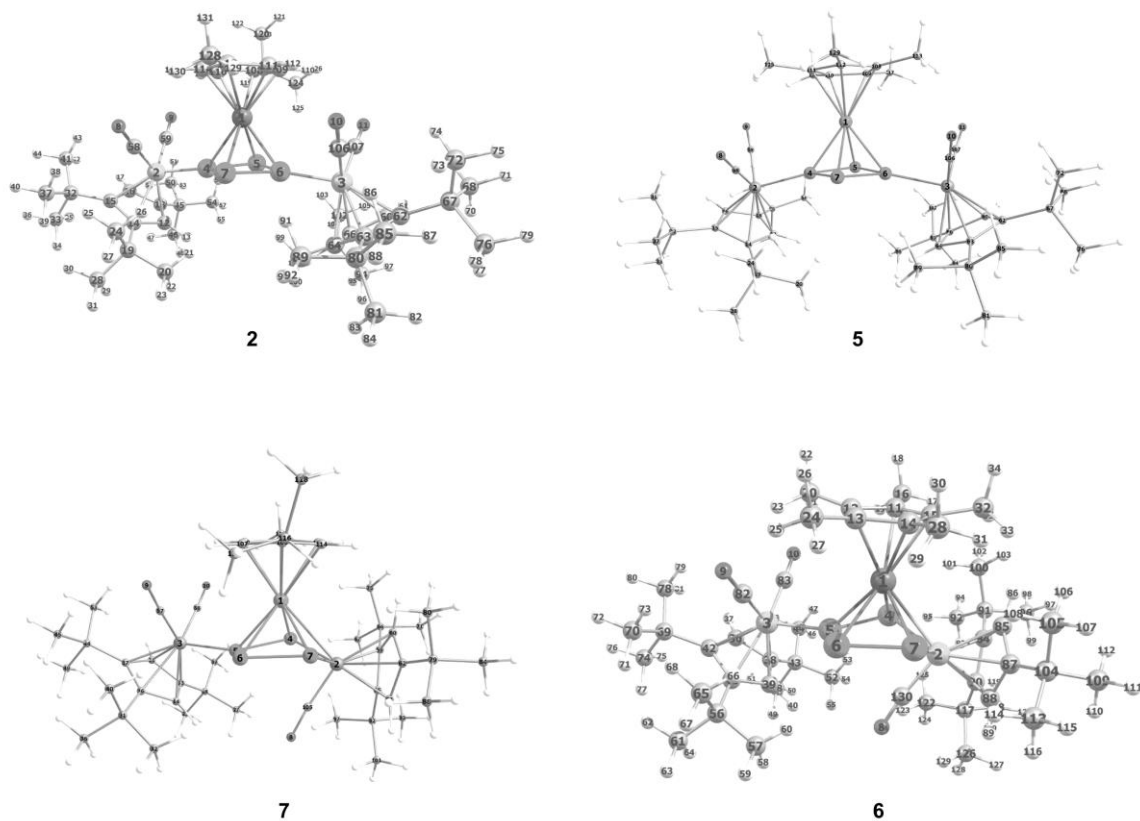


Figure S26. Optimized structure of $[\{\text{Cp}^{\text{III}}\text{Fe}(\text{CO})_2\}_2(\mu_3, \eta^{4:1:1}\text{-P}_4)(\text{CymRu})]^{2+}$ (**2**), $[\{\text{Cp}^{\text{III}}\text{Fe}(\text{CO})_2\}_2(\mu_3, \eta^{4:1:1}\text{-P}_4)(\text{Cp}^*\text{Ru})]^{+}$ (**5**), $[\{\text{Cp}^{\text{III}}\text{Fe}(\text{CO})_2\}\{\text{Cp}^{\text{III}}\text{Fe}(\text{CO})\}(\mu_3, \eta^{4:2:1}\text{-P}_4)(\text{CymRu})]^{2+}$ (**7**) and $[\{\text{Cp}^{\text{III}}\text{Fe}(\text{CO})_2\}\{\text{Cp}^{\text{III}}\text{Fe}(\text{CO})\}(\mu_3, \eta^{4:2:1}\text{-P}_4)(\text{Cp}^*\text{Ru})]^{+}$ (**6**) with the atom assignment.

Table S9. Calculated total energy of complexes **2**, **5**, **6**, **7** and CO.

	5	6	2	7	CO
BP86/def2-TZVP					
Tot. E [au]	-6163.618	-6050.2167	-6162.736	-6049.308	-113.365
Tot. E [kJ/mol]	-16182579.092	-15884843.558	-16180261.959	-15882457.721	-297640.623
B3LYP/def2-TZVP; COSMO (acetonitrile)					
Tot. E. [a.u.]	-6160.950	-6047.602	-6160.191	-6046.823	-113.311
Tot. E. [kJ/mol]	-16175573.423	-15877979.547	-16173582.450	-15875933.929	-297497.986
Tot E. + OC corr [au]	-6160.945	-6047.598	-6160.184	-6046.815	-113.311
Tot E. + OC corr [kJ/mol]	-16175561.872	-15877967.975	-16173562.440	-15875913.548	-297498.024

Table S10. Calculated reaction energies at the SP-COSMO-B3LYP level of the transformation of **5** to **6** and **2** to **7**.

Reaction	Reaction energy [kJ/mol]
$[\{\text{Cp}^{\text{III}}\text{Fe}(\text{CO})_2\}_2(\mu_3, \eta^{4:1:1}\text{-P}_4)(\text{Cp}^*\text{Ru})]^{+} \rightarrow [\{\text{Cp}^{\text{III}}\text{Fe}(\text{CO})_2\}\{\text{Cp}^{\text{III}}\text{Fe}(\text{CO})\}(\mu_3, \eta^{4:2:1}\text{-P}_4)(\text{Cp}^*\text{Ru})]^{+} + \text{CO}$	95.87
$[\{\text{Cp}^{\text{III}}\text{Fe}(\text{CO})_2\}_2(\mu_3, \eta^{4:1:1}\text{-P}_4)(\text{CymRu})]^{2+} \rightarrow [\{\text{Cp}^{\text{III}}\text{Fe}(\text{CO})_2\}\{\text{Cp}^{\text{III}}\text{Fe}(\text{CO})\}(\mu_3, \eta^{4:2:1}\text{-P}_4)(\text{CymRu})]^{2+} + \text{CO}$	150.87

Table S11. Selected Wiberg bond indices for $[\{\text{Cp}^*\text{Fe}(\text{CO})_2\}\{\text{Cp}^*\text{Fe}(\text{CO})\}(\mu_3, \eta^{4:2:1}\text{-P}_4)(\text{Cp}^*\text{Ru})]^+$ (**6**).

Fe2 - Ru1	0.317	P4 - Ru1	1.015	P5 - P4	0.974
P4 - Fe2	0.796	P5 - Ru1	0.604	P6 - P5	1.012
P5 - Fe3	0.970	P6 - Ru1	0.742	P7 - P6	1.127
P7 - Fe2	0.768	P7 - Ru1	1.082	P7 ... P4	0.029

5. Literature:

- [1] C. Schwarzmaier, A. Y. Timoshkin, G. Balázs, M. Scheer, *Angew. Chem. Int. Ed.* **2014**, *53*, 9077.
- [2] F. Kleinbeck, G. J. Fettes, L. D. Fader, E. M. Carreira, *Chem. Eur. J.* **2012**, *18*, 3598.
- [3] *CrysAlisPro Software System*, Agilent Technologies UK Ltd, Yarnton, Oxford, **2014**.
- [4] G. Sheldrick, *Acta Cryst. A* **2015**, *71*, 3.
- [5] G. M. Sheldrick, *Acta Cryst. A* **2015**, *71*, 3.
- [6] O. V. Dolomanov, L. J. Bourhis, R. J. Gildea, J. A. K. Howard, H. Puschmann, *J. Appl. Crystallogr.* **2009**, *42*, 339.
- [7] a) R. Ahlrichs, M. Bär, M. Häser, H. Horn, C. Kölmel, *Chem. Phys. Lett.* **1989**, *162*, 165; b) O. Treutler, R. Ahlrichs, *J. Chem. Phys.* **1995**, *102*, 346.
- [8] K. Eichkorn, O. Treutler, H. Öhm, M. Häser, R. Ahlrichs, *Chem. Phys. Lett.* **1995**, *242*, 652.
- [9] K. Eichkorn, F. Weigend, O. Treutler, R. Ahlrichs, *Theor. Chem. Acc.* **1997**, *97*, 119.
- [10] a) P. A. M. Dirac, *Proceedings of the Royal Society of London. Series A* **1929**, *123*, 714; b) J. C. Slater, *Physical Review* **1951**, *81*, 385; c) S. H. Vosko, L. Wilk, M. Nusair, *Can. J. Phys.* **1980**, *58*, 1200; d) A. D. Becke, *Physical Review A* **1988**, *38*, 3098; e) J. P. Perdew, *Physical Review B* **1986**, *33*, 8822; f) J. P. Perdew, *Physical Review B* **1986**, *34*, 7406.
- [11] A. Schäfer, C. Huber, R. Ahlrichs, *J. Chem. Phys.* **1994**, *100*, 5829.
- [12] M. Sierka, A. Hogekamp, R. Ahlrichs, *J. Chem. Phys.* **2003**, *118*, 9136.